# CATALYTIC PYROLYSIS OF VIRGIN AND WASTE POLYOLEFINS

**A Thesis Submitted to the Graduate School of Engineering and Sciences of İzmir Institute of Technology in Partial Fulfilment of the Requirements for the Degree of**
**MASTER OF SCIENCE**
**in Energy Engineering**

**by**
**Fatma Defne ÇALIK**

**June 2023**
**İZMİR**

We approve the thesis of **Fatma Defne ÇALIK**

**Examining Committee Members:**

**Prof. Dr. Jale YANIK**
Chemistry, Ege University

**Asst. Prof. Dr. Başar ÇAĞLAR**
Energy Systems Engineering, İzmir Institute of Technology

**Asst. Prof. Dr. Güray YILDIZ**
Energy Systems Engineering, İzmir Institute of Technology

**23 June 2023**

**Asst. Prof. Dr. Güray YILDIZ**
Supervisor, Energy Systems Engineering,
İzmir Institute of Technology

**Prof. Dr. Erol ŞEKER**
Co-Supervisor, Chemical Engineering
İzmir Institute of Technology

**Prof. Dr. Gülden Gökçen AKKURT**
Head of the Department of Energy Systems Engineering

**Prof. Dr. Mustafa DEMİR**
Dean of the Graduate School of Engineering and Sciences

# ACKNOWLEDGMENTS

First of all, I would like to thank my thesis supervisor Asst. Prof. Dr. Güray Yıldız for all his support and encouragement during my master's degree. At the same time, I would like to thank my co-advisor Prof. Dr. Erol Şeker for his guidance and understanding. I would also like to thank my advisor Assoc. Prof. Dr. Monika Kalinowska, who gave me every opportunity to learn characterization techniques and gain lab experience during my Erasmus internship at Bialystok University of Technology.

This work is supported and funded by the UK Department for Business, Energy and Industrial Strategy together with the Scientific and Technological Research Council of Turkey (TÜBİTAK; Project No. 119N302) and delivered by the British Council.

I would like to thank to members of the Laboratory of Thermochemical Conversion Technologies, Ecrin Ekici, Gülsün Gizem Taylan, and Nazire Merve Akbaş, for being more than colleagues. I am thankful for the support of the Renewable Energy and Hydrogen Research Laboratory for catalyst production. Also, I would like to express my sincere feelings for my teammates Cem Karacasulu, Emre Değirmenci and Özgür Enes Taytaş in the chemical engineering department for their help to prepare ex-situ catalytic pyrolysis set-up. I would like to thank the Izmir Institute of Technology Integrated Research Center for helping me analyze the raw materials and products during my thesis work.

I would like to thank my two closest friends, Süleyman Burçak Çıkıkçı and Şebnem Kılıç, beyond the siblings I had during my undergraduate and graduate studies. I would like to thank my dear family for their endless love and support throughout my entire education life. Finally, I would like to thank my precious fiancé Anılcan Ulu for believing in me, growing with me and for his never-ending love, I could not have succeeded without him.

# ABSTRACT


## CATALYTIC PYROLYSIS OF VIRGIN AND WASTE POLYOLEFINS

The fact that increasing plastic production and the mismanaged waste released to the environment put the ecosystem at risk. One of the most promising recycling methods developed within this framework has been pyrolysis. In this thesis, a model feedstock mixture was prepared in proportion to the plastic packaging waste collected from İzmir within the scope of a TÜBİTAK project (No: 119N302). Thermal (batch and continuous) and catalytic pyrolysis (in-situ and ex-situ) techniques were applied to the polyolefins. Silica-alumina-based solid acid catalysts were produced with the simple sol-gel method to compete with commercial ZSM-5 (30) and ZSM-5 (50). Catalyst-to-plastic ratios between 1/100 and 1/1000 were used for in-situ, and 200 $h^{-1}$ and 500 $h^{-1}$ WHSVs were used for ex-situ mode. 57 wt.% pyrolysis oil was produced from the thermal pyrolysis of the virgin PO mixture in the batch system. In the ex-situ catalytic pyrolysis experiments by 500 $h^{-1}$ WHSV and by ZSM-5, silica-alumina, and ZSM-5 supported silica-alumina, 36 wt.%, 56.6% wt.% and 45.2 wt.% liquid, and by 200 $h^{-1}$ WHSV, 29.9 wt.%, 54.1 wt.%, and 57.9 wt.% pyrolysis oils were collected, respectively. The most successful test in terms of product composition was ES2 with 82.9% gasoline (8.8% BTEX), and 16.7% diesel-range hydrocarbons. The motivation was investigating whether it was suitable to produce liquid hydrocarbons, in the range of $C_5$-$C_{20}$, as a feedstock in the petrochemical industry. As a result, it has been proven that energy recovery was possible and sustainable by plastics recycling instead of using fossil fuels.

# ÖZET

## İŞLENMEMİŞ VE ATIK POLİOLEFİNLERİN KATALİTİK PİROLİZİ

Gün geçtikçe artan plastik üretiminin ve açığa çıkan atıkların iyi yönetilememesi çevre ve insan sağlığını tehlikeye atmaktadır. Bu çerçevede geliştirilen ve en umut vaat eden geri dönüşüm metodlarından biri pirolizdir. Bu tez çalışmasında, TÜBİTAK projesi (No: 119N302) kapsamında İzmir'den toplanan plastik ambalaj atıklarının oranında model hammadde karışımı hazırlandı. Poliolefinlere termal (kesikli ve sürekli) ve katalitik piroliz (in-situ ve ex-situ) teknikleri uygulandı. ZSM-5 (30) ve ZSM-5 (50) ile rekabet edebilmek için basit sol-jel yöntemiyle silica-alumina bazlı katı asit katalizörleri üretildi. In-situ için 1/100 ve 1/1000 arasındaki katalizör/plastik oranları ve ex-situ mod için 200 $h^{-1}$ ve 500 $h^{-1}$ WHSV'ler kullanıldı. Kesikli sistemde işlenmemiş PO karışımının termal pirolizinden ağırlıkça %57 piroliz yağı üretildi. 500 $h^{-1}$ WHSV ile yapılan ex-situ katalitik piroliz deneylerinde, ZSM-5, silica-alumina ve ZSM-5 destekli silica-alumina, ağırlıkça %36, %56,6 ve %45,2 sıvı elde edilmesini sağladı. 200 $h^{-1}$ WHSV ile sırasıyla ağırlıkça %29.9, %54.1 ve %57.9 piroliz yağları toplandı. Ürünün kimyasal içeriği açısından en başarılı deney, %82,9 gasoline (%8,8 BTEX) ve %16,7 diesel kalitesinde hidrokarbon içeren ES2 oldu. Bu tezdeki amaç $C_5$-$C_{20}$ aralığında gasoline ve diesel hidrokarbonlarını üretip petrokimya endüstrisinde hammadde olarak kullanılmaya uygun olup olmadığını araştırmaktı. Bu çalışmadan elde edilen sonuçların ortaya koyduğu üzere, fosil yakıtları kullanmak yerine geri dönüşümle enerji kazanımının mümkünlüğü ve sürdürülebilirliği kanıtlanmış oldu.

# TABLE OF CONTENTS

# LIST OF FIGURES

# LIST OF TABLES

**Table** **Page**

# CHAPTER 1

# INTRODUCTION

The increasing human population in the world brings with it some needs and problems due to urbanization and industrialization. One of them is the environmental problems created by waste (paper, plastic, glass, metal etc.) that are released in uncontrolled amounts. When efficient and planned waste management cannot be provided, the garbage stored in nature affects water, soil and the entire ecosystem. Uncontrolled waste thrown into the environment pollutes the air, water and soil with its toxic additives. Greenhouse gases are released during the uncontrolled burning or storage of this garbage. Therefore, carbon emissions have considerably increased. Another issue is the increasing energy demand. In addition to these, the depletion of fossil resources has also created a demand for new energy production methods. The aim of taking measures against global warming, protecting the ecosystem, and meeting the energy need at the same time, led scientists to find routes for renewable energy and sustainability. It is aimed to provide a more sustainable life by choosing recycling, recovery, reduce and reuse methods according to the suitability of the waste type (Sakthipriya 2022). Many waste management methods have been developed to supply sustainability. Thus, valuable chemicals and fuels to be obtained from waste will be produced without the need for fossil resources. This transition from cradle-to-grave (one way flow) to cradle-to-cradle (closed loop cycles) behaviour will also positively contribute to the circular economy (El-Haggar 2007).

Worldwide solid waste generation has been obtained as 29% organics, 9% inorganics, 18% paper, 13% plastic, 9% textile, 9% metals, 4% glass and other wastes is 9% by 2020. 370 million tons of plastics were produced globally in 2020 (M.I. Jahirul 2022). These plastics are produced and used in sectors such as transportation, textiles, packaging, industrial machinery, electrical/electronic, consumer & institutional products, building and construction, and others (Chang 2023, M.I. Jahirul 2022). The most striking sector is packaging, with a production of approximately 141 million tons and use of 138 million tons (M.I. Jahirul 2022). The top 10 countries in the amount of waste generated per capita in 2020 are the United States, the United Kingdom, South Korea, Germany, Thailand, Malaysia, Argentina, Russia, Italy and Brazil. These amounts range from 105.3

kg/year to 51.78 kg/year (Chang 2023). When the energy and environmental statistics of 27 countries included in the European Union are examined (EU-27) it is seen that 492 kg/year of municipal solid waste (MSW) per capita were produced in 2017. The majority of MSW, 173.8 kg/year, consists of packaging materials (41% paper & cardboard, 19% plastic, 18% glass, 17% wood, and 5% metal). The plastic packaging waste amount was determined as 32.6 kg/year per person. The targeted plastic packaging recycling (plastics to plastics) rate of 22.5% has reached an average of 41.7%, excluding one country (Eurostat 2020). When examined in Europe, 42% of the 17.8 million tons of used packaging waste collected in 2018 was recycled, 39.5% was used in energy recovery and 18.5% was sent to landfill (Marvin Kusenberg 2022).

In Turkey, packaging waste consists of 25% plastic, 3.5% metal, 2.6% composite, 32.3% paper-cardboard, 21.6% glass and 15% wood. While 62.1% of the total packaging waste was recovered, 66.5% of the plastic packaging waste was recovered (Ministry of Environment 2020). Plastic packaging production covers approximately 3.08 million tons of 7.3 million tons of plastic production in the first 9 months of 2020 (PAGEV 2020). In the province of İzmir, which narrows down the examined environment and forms the scope of this thesis, it is observed that the content of packaging waste is 8.2% plastic, 0.8% metal, 11.2% composite, 27.6% paper-cardboard, 42.3% glass and 9.9% wood. The recycling rate of plastic packaging in İzmir has reached 32.2% (PROVINCIAL DIRECTORATE OF ENVIRONMENT 2021).

As mentioned, plastic materials are used in various sectors. The plastic packaging used here constitutes especially food & cleaning containers, as well as disposable products brought with it by the COVID-19 pandemic. These materials mentioned are thermoplastic polymers. According to resin identification codes (RIC), they are classified as 1 polyethylene terephthalate (PET), 2 high-density polyethylene (HDPE), 3 polyvinyl chloride (PVC), 4 low-density polyethylene (LDPE), 5 polypropylene (PP), 6 polystyrene (PS)), and 7 other resins (OTHERS) (Chang 2023, Charlotte Abdy 2022, Vahid Mortezaeikia 2021). Polyolefins are the special name of the group formed by polyethylenes, $(C_2H_4)_n$, and polypropylene, $(C_3H_6)_n$, (HDPE, LDPE, PP) (Dylan Jubinville 2020). HDPE polymer is crystalline because of its linear and unbranched chemical structure and has high intermolecular force. Thus, its tensile strength is high. LDPE, on the other hand, is the branched version of HDPE and therefore has lower intermolecular force compared to it. The result is a more ductile material with lower tensile strength. Polypropylene is a highly tough material and has low density (Lesli O.

Mark 2020). Polyolefins constitute a large part of the household plastic waste (HPW) content. HDPE is used for detergent, milk and oil bottles, buckets, slides, trash cans, and toys, while LDPE is used for plastic bags, plastic food wraps, kitchen appliances, dispensing bottles, wash bottles, squeeze bottles, tubing and computer components. And, PP is used for plastic furniture, medical devices, packaging trays, car bumpers, storage boxes, battery cases, carpets, food and laboratory appliances and household products (M.I. Jahirul 2022, Chang 2023).

Large amounts of plastic waste are mostly irregularly discharged into nature or landfilled. Innovative methods have been developed to recycle plastic materials with various properties and their additives without endangering the ecosystem and human health. Fan Zhang divided these methods into recycling and degradation under the title of advanced nonbiodegradable plastic waste (NPW) disposal methods. Recycling has been examined as physical recycling, energy recovery (incineration) and resource recovery (thermolysis, chemolysis) according to certain ASTM standards. Physical recycling methods consist of extrusion, segregation, reuse etc. (Fan Zhang 2021). Martyna Solis classified recycling methods as primary, secondary (mechanical recycling), tertiary (thermochemical recycling), and quaternary recycling (incineration). Primary recycling is the continuation of the use of plastic of the same quality without changing. With the secondary recycling method, the quality of the plastic is changed by mechanical degradation (Martyna Solis 2020). Sakthipriya examined recycling under three separate headings: physical (UV treatment, photooxidation, size reduction), thermochemical and biological (composting, anaerobic digestion, fermentation) (Sakthipriya 2022).

The most effective and suitable methods for recycling polymers are thermochemical methods. By providing monomer recovery, valuable chemicals and fuel production, a more sustainable process is realized, and it is possible to fill a large gap in energy needs. One of the most widely used methods is incineration, which allows wastes to be burned at high temperatures in a controlled manner, releasing heat, that is, energy recovery. One of the most important reasons for this preference is that plastics have a calorific value almost identical to petrochemical products (i.e. fuels) (Fan Zhang 2021). However, during this, many harmful gases (i.e. $CO_2$, $NO_x$) are released into nature. For this reason, it is recommended to use other thermochemical methods such as pyrolysis and gasification, which will reduce the carbon emission. Thermolysis (heterogeneous) and chemolysis (homogeneous) methods are used to provide resource recovery. Chemolysis, solvolysis or depolymerization enables individual plastics to be broken

down into monomers (monomer recovery) by applying chemical treatment at 80-280 °C temperatures. Hydrocracking, or hydrogenation, takes place under high pressure (i.e. 70 atm) and in the temperature range of 375-500 °C. By adding hydrogen to the system, long hydrocarbon chains are broken and gasoline-kerosene range hydrocarbons can be obtained. Gasification takes place using gasifying agents such as air, steam or plasma in the temperature range of 700-1200 °C. The goal is to produce syngas (i.e. $CO_2$, CO, $H_2$, $CH_4$, light hydrocarbons) and the by-products are tar and char. Hydrocracking and gasification are not cost-effective due to the hydrogen gas used or the high-temperature requirements (Fan Zhang 2021, Martyna Solis 2020).

In this master's thesis, the thermal and catalytic pyrolysis processes of polyolefins (individually and as a mixture) were investigated through different process parameters. Batch and continuously operated reactors were investigated and compared. Also, the behaviour of the catalyst contact mode, in situ and ex-situ, was researched. Silica-alumina catalysts were developed and the conversion and selectivity values of different catalysts with different catalyst-to-plastic ratios were compared. This research aimed to maximize the liquid production in the $C_5$-$C_{20}$ range by providing fast pyrolysis conditions. For this, nonviscous pyrolysis oils were produced with various amounts and a variety of catalysts. The content of the products obtained from this study was analyzed by characterization techniques (i.e. GC, FTIR) and it was observed that they can be suitable for use as raw materials in the petrochemical industry.

# CHAPTER 2

# THERMAL AND CATALYTIC PYROLYSIS OF POLYOLEFINS

The process examined in detail in this thesis is the pyrolysis method. Pyrolysis is the process of breaking the raw materials into small pieces by providing an inert atmosphere (oxygen-free environment) through gases such as $N_2$, He, Ar, in the temperature range of 300-700 °C. It is usually performed under atmospheric pressure. It is a suitable method for many types of plastics (individual/mixture), especially polyolefins. Pyrolysis oil, noncondensable gas and char are obtained from the pyrolysis of plastics. Depending on whether the pyrolysis takes place fast or slow, the liquid or solid product is favoured. Certain process parameters are used to provide good thermochemical cracking and increase the yield and selectivity of the product. These are temperature, heating rate, residence time, inert gas flow rate, pressure, reactor types and configuration (batch-semi batch, continuous operation), feedstock and catalyst type, catalyst contact mode, catalyst-to-plastic ratio, and space-time (Fan Zhang 2021).

The temperature factor directly affects the yield of the product. It must be at a certain height for cracking to occur, but an optimum condition must be set to increase the amount of liquid. Because as the temperature increases, gas production will increase at the same time. After the melting and maximum cracking temperature values for each plastic are determined by performing TGA and DSC analyzes, the process temperature should be determined. In addition, the temperature ranges can be narrowed to 450-600 °C depending on the content of the targeted product (i.e. aromatics production) (Mehrdad Seifali Abbas-Abadi 2023, Ijaz Hussain 2022). With a high heating rate (10-200 °C/s), the raw material is brought to the target pyrolysis temperature quickly and the majority of the product can be obtained as a liquid. Feedstock residence time and heating rate are factors that affect each other inversely. If the heating rate increases, the feedstock residence time decreases, and secondary cracking reactions are prevented. Thus, the liquid product is maximized (Mehrdad Seifali Abbas-Abadi 2023, Tu Xayachak 2022). Another factor associated with residence time is the inert gas flow rate (also called fluidizing gas). As the inert gas flow rate used to transport the pyrolysis vapour from the reactor to the condenser increases, the vapour residence time decreases. Thus, secondary

cracking and the amount of light olefin gas production are prevented (Mehrdad Seifali Abbas-Abadi 2023, Fan Zhang 2021).

There is not as much research on the pressure effect as on other parameters, but it is possible to increase product efficiency by changing other parameters as the pressure changes. In some studies, it has been observed that pyrolysis working under a vacuum reduces the process temperature. And it has been determined that, when considering product yield, the pressure change is more effective at low pyrolysis temperatures compared to the high temperature. In addition, it was observed that while heavy hydrocarbons (heavy oil) were obtained in experiments performed under low pressure, lighter hydrocarbons (oil and gas) were obtained as the pressure increased. Besides, the use of high pressure has been proposed to provide aromatic production (Fan Zhang 2021, Tu Xayachak 2022, Ijaz Hussain 2022, F. Faisal 2023). As mentioned in the study of Ijaz Hussain et al., the effect of pressure has an important place in the catalyst activity (Ijaz Hussain 2022).

The type of feedstock used is important because its content and chemical structure gives information about how it will react and what it will produce as a result. For example, PVC produces HCl due to its chlorine content and the resulting liquid quality is low. For this reason, pretreatment such as dechlorination/deoxygenation is required for these types of (i.e. PET, PVC) plastics. However, working with polyolefins or polystyrene, the content of only carbon and hydrogen is more suitable for pyrolysis. In addition, the melting points, boiling points, and maximum degradation temperatures of these plastics are also different from each other. The behaviour of the mixture pyrolysis will vary with the plastic pyrolysis applied individually (Fan Zhang 2021, F. Faisal 2023, S. Kartik 2022). From the pyrolysis of HDPE plastic, primarily paraffinic waxes, and α-olefins, and also some benzene, toluene, xylene (BTX) and some cyclic compounds (i.e. cyclohexene) are obtained. LDPE likewise converts primarily to paraffinic waxes, and α-olefins, and secondarily to aromatic hydrocarbons such as BTX and naphthalene. PP polymer primarily produces short-chain alkenes & alkanes, and olefins, as well as aromatics of benzene, toluene, ethylbenzene, and xylene (BTEX) (Tu Xayachak 2022, R. Miandad 2017).

The type of pyrolysis reactor, which is the most important part of the pyrolysis method, and the mode of operation are the parameters that should be carefully selected. Reactor types used for pyrolysis in the literature, batch & semi-batch lab-scale reactors, continuous flow reactors (fixed and fluidized bed), lab-scale conical spouted bed reactors

(CSBR), two-stage pyrolysis systems (fixed bed and CSBR), stirred reactors, fluid catalytic cracking (FCC) units are microwave-assisted pyrolysis (MAP), plasma-assisted pyrolysis, screw kiln, molten bath, pyrolysis in supercritical water (SCW), and gas-solid vortex reactors (Lesli O. Mark 2020, Fan Zhang 2021, D. P. Serrano 2012, A.G. Buekens 1998, S.L. Wong 2015, Gartzen Lopez 2017, Ina Vollmer 2020). The reaction can be performed in batch, semi-batch, or continuous systems. In batch mode, there is no entry or exit from the system. The plastic raw material is placed in the system beforehand the reaction is started. As a result of the experiment, the liquid product accumulated in the flask is collected and taken for analysis. Two methods can be used in the semi-batch operation. Feedstock is fed into the system, the product accumulates in the flask, or the feedstock is pre-placed in the reactor, but a continuous flow (liquid, noncondensable gas) is observed out of the system. The system, which works in continuous mode, includes a feeding unit and raw materials are added at regular intervals. As the reaction takes place, the resulting fluid products are continuously collected from outside the system and analyzed (GC).

Batch & semi-batch lab scale reactors are advantageous in terms of frequent material charging and restarting of the process. They provide easy control of the parameters and high liquid yields. However, because heat & mass transfer is poor and the available catalytic surface area for reactants to access is limited, it has been necessary to develop more suitable reactors for the process, since coke formation is present (Lesli O. Mark 2020, D. P. Serrano 2012, Fan Zhang 2021, S.L. Wong 2015). Likewise, in lab-scale fixed bed reactors, the surface area of the catalyst is limited in catalytic reactions and also reactor blockages occur due to the inefficiency of heat & mass transfer. The volume limitations of these reactors should be eliminated to use them in commercial applications. For this reason, it is generally used as a secondary reactor with other reactors (Lesli O. Mark 2020, D. P. Serrano 2012, Fan Zhang 2021, S.L. Wong 2015, Gartzen Lopez 2017). Fluidized bed reactors are reactors that can adapt to both lab scale and industrial scale. Providing good heat & mass transfer, excellent mixing, high heating rates, easy changing fluidizing flow rate, and no need to recharge & restart materials are its biggest advantages. Thus, secondary reactions can be minimized, and labour costs can be reduced by providing isothermal beds and short residence times. However, its negative properties such as defluidization problems, feedstock preparation required for industrial pyrolysis, and the need for catalyst regeneration also need to be resolved (Lesli O. Mark 2020, D. P. Serrano 2012, A.G. Buekens 1998, Fan Zhang 2021, S.L. Wong 2015,

Gartzen Lopez 2017, Ina Vollmer 2020). Lab-scale conical spouted bed reactors (CSBR) have a lower chance of agglomeration, defluidization and lower pressure drop than fluidized beds. They can supply high heat and mass transfer rates, good mixing capabilities, and vigorous gas-solid contact. They can provide short vapour residence time and prevents secondary reactions and coke formation. CSBRs allow operating with catalysts in in-situ mode. However, these are selective for the high-weight waxes so there is a need for a second reactor (Lesli O. Mark 2020, D. P. Serrano 2012, Fan Zhang 2021, S.L. Wong 2015, Gartzen Lopez 2017, Ina Vollmer 2020). Two-stage pyrolysis systems are designed to break the wax produced with CSBR into smaller hydrocarbons. Secondary fixed bed reactors are preferred because of their opportunity for scale-up, lower operating temperature for catalytic bed, and less/no reactor blockages. Thanks to the ex-situ catalyst mode, which can be used, easier catalyst recovery can be achieved and direct contact of plastics with catalysts can be prevented (Lesli O. Mark 2020, S.L. Wong 2015).

Heat transfer is very successful as stirred reactors allow the plastic to melt by mixing. At the same time, it is one of the most practical alternative reactors because it can work in both batch and continuous operation modes (Gartzen Lopez 2017). Fluid catalytic cracking (FCC) units are among the successful reactors known for their frequent use in the industry which is compatible with continuous operation. It provides to reduce the viscosity of the feedstock. To overcome the continuous feeding of solid plastic, a suitable solvent is used and then the pyrolysis process is performed. It is possible to separate mixed plastic waste into their components and contaminants can be removed by using selective dissolution. In addition, pretreatment is needed before feeding into the feedstock to the FCC unit (D. P. Serrano 2012, S.L. Wong 2015, Ina Vollmer 2020). Microwave-assisted pyrolysis (MAP) is a cost-effective technique that can provide fast and selective heating and easy control of reaction conditions. Its higher microwave power caused more efficient degradation (S.L. Wong 2015, Gartzen Lopez 2017, Ina Vollmer 2020). Plasma-assisted pyrolysis is also capable of providing rapid heating to high temperatures and extremely high heating rates. So, it can approximately double the monomer recovery rates, promotes almost full tar cracking (for gasification), and therefore end up with high gas yields (Ina Vollmer 2020). The screw kiln reactor is simply designed and is proper for scaling up. Residence time can be arranged by screw speed. It can provide a good heat transfer rate and control solid residence time & pyrolysis temperature. There is good mixing that can be provided, and no limitation on particle size. There is intimate contact between the primary cracking products and the catalyst. Nevertheless, there is easy

catalyst removal & polymer handling. Also, it can be operated in a continuous regime, but maintenance costs will be high. Heat efficiency is low, therefore heavy hydrocarbons are produced (D. P. Serrano 2012, Gartzen Lopez 2017, Ina Vollmer 2020).

For molten bath reactors, there is direct contact between the polymer and the molten metal. Also, they provide a high heat transfer rate, good control of temperature and no limitation on particle size. Continuous operation can be performed but the material cost is high, and it is difficult to startup, shutdown, and scale up (Gartzen Lopez 2017). Supercritical water behaves as a solvent and catalyst for pyrolysis in the SCW technique. Subsequent condensation and coke formation chance is lower with SCW. And excellent property of debromination can be performed. Also, a negligible amount of $NO_x$, $SO_x$ and particulate emission is possible (S.L. Wong 2015). Another type of pyrolysis reactor, the gas-solid vortex reactor, has also been developed to overcome heat and mass transfer limitations (Ina Vollmer 2020).

The technique in which catalysts are included in thermal pyrolysis is called catalytic pyrolysis (CP). Catalytic pyrolysis takes place in two different catalyst contact modes, in-situ and ex-situ. In-situ mode is when the plastic raw material and the catalyst are in direct contact in the same reactor while the pyrolysis reaction takes place. In the ex-situ CP mode, first of all, pyrolysis vapours are produced in the thermal pyrolysis reactor and these vapours come into contact with the catalyst in another reactor. Thus, the contact of all the pyrolysis vapour with the catalyst is carried out equally and more selective products are obtained. The important operation parameters, which are also examined for the yield and content of the products to be obtained from catalytic pyrolysis, are catalyst type, catalyst-to-plastic ratio, and space-time (Yildiz G. 2017). Factors such as catalyst-to-plastic ratio and space-time are used to examine the product yield and selectivity with the effects of catalyst and plastic amounts, inert gas flow rate, and plastic feeding rate on each other (Lesli O. Mark 2020, Yujie Peng 2022, Haoran Yuan 2022).

Undoubtedly, the most important factor of catalytic pyrolysis is the types of catalysts. In the literature, there are many types of catalysts were researched for the catalytic pyrolysis of plastics, especially zeolites. Both homogeneous (i.e. Lewis acids) and heterogeneous catalysts were used for plastics recycling. For easy separation of catalyst and a pyrolysis liquid mixture, the most commonly used catalysts are the heterogeneous ones. Heterogeneous catalysts are more desirable due to their capability to convert plastic solid waste into valuable liquid and gaseous hydrocarbons (HCs). Catalyst acidity and pore structure are important parameters that can be arranged to increase

product selectivity. Heterogeneous catalysts utilized for the CP of plastics are amorphous silica-alumina, mesoporous silica, mesoporous silica-alumina, FCC catalysts, activated carbon, clays, metal oxides, carbonates, zeolite Y, ZSM-5, β-zeolite, and natural zeolites (Lesli O. Mark 2020).

Amorphous silica-alumina catalysts provide bond activation for solid plastic waste molecules, so polymer decomposition becomes faster. They provide an increase in product distribution & quality and reduce residue formation. There is a tunable acidity property when alumina increase, acidity increases. Lower acid content supplies high liquid selectivity. Mesoporous silica and mesoporous silica-alumina catalysts are improved by their pore structures. Their pore structure improves diffusion and faster cracking. If the acidity becomes lower, there is an enhanced catalytic cracking, inhibition of secondary cracking, and liquid yield increase for kerosene and diesel fractions. FCC catalysts consist of crystalline zeolites with some binders and promoters. They can provide $C_{13}$-$C_{20}$ hydrocarbon selectivity. Low-acidic catalyst reactions end up with less aromatic and more olefinic naphtha. If the catalyst is strongly acidic, the highest amount of hydrocarbons will be including $C_5$-$C_6$ olefins but with coke formation (Lesli O. Mark 2020).

Activated carbons have a large surface area and high heat transfer area, so selectivity will be decreased. Their acidity can be tuned by -OH, -OOH, and -P-O. By using a weakly acidic activated carbon jet fuel range alkanes are favoured while stronger acidity favours jet fuel range aromatics. Clays are weaker acidic catalysts. Diesel fuel production from plastic solid waste (PSW) can be possible with a microporous structure and milder acidity. The macroporous structure provides inhibition of polymers with active sites, and desorption and no further reactions can occur. Milder acidity improves catalytic polymer cracking for heavier pyrolysis products. Metal oxides with moderate acidity improve liquid yield with high selectivity towards olefinic and naphthenic compounds. Noble metals can be supported by metal oxides for producing gasoline and diesel range hydrocarbons. Carbonates are thermally instable catalysts. To increase the rate of plastic degradation, they can reduce operational temperature and residence time. For example, $MgCO_3$ for HDPE ends up with pyrolysis oil including high diesel, and a small amount of gasoline (Lesli O. Mark 2020).

Zeolite Y (faujasite, HY, USY, HUSY) provides high selectivity for lowering olefin content and increasing light hydrocarbons such as gasoline and diesel fuels. This catalyst is thermally stable and has acid site accessibility to enhance catalytic cracking.

By changing Si/Al ratio acidity can be arranged. Higher acidity can be reached by lowering the Si/Al ratio and provide having higher yields of aromatic and olefin compounds. Large pores of this catalyst help increase the product distribution, but heavier HCs and coke can be formed. ZSM-5 catalyst consists of smaller pores in combination with strongly acidic sites. It is highly active in cracking for polyolefins, especially polyethylenes (PE). For PEs lower heavy oil, minimum char formation and higher light HC content in liquid can be performed and generally, light alkene and aromatics are produced. For nanocrystalline zeolites, selectivity is effective on a smaller range of carbon numbers $C_1$-$C_5$, especially $C_3$-$C_5$. β-zeolites can increase gas fractions and reduce liquid oil. Its acidity can be arranged by changing Al with a variety of metals and it is highly dependent on the amount of highly acidic Si(OH)Al groups. Natural zeolites (i.e. mordenite, clinoptilolite) are naturally occurring silica-rich zeolites. They are readily available and inexpensive. Besides, they contain impurities such as Na, Mg, S, K, Ca, Ti, and Fe which can cause further reactions. Protonated natural zeolites improved both the yield of liquid and char thanks to moderate cracking (Lesli O. Mark 2020).

The general catalytic polymer degradation mechanism includes initiation, second-step reactions, and termination. Firstly, protonation or hydride abstraction of polymer can be performed to obtain carbenium ions. Later, carbenium ion can undergo second step reactions which are β-scission, isomerization or hydrogen transfer reactions. After obtaining primary and secondary unstable molecular fragments, the termination step can be performed by the recombination, disproportionation, cyclization, aromatization or polycondensation reactions (Luis Noreña 2011, Sachin Kumar 2011) (Figure 2.1).

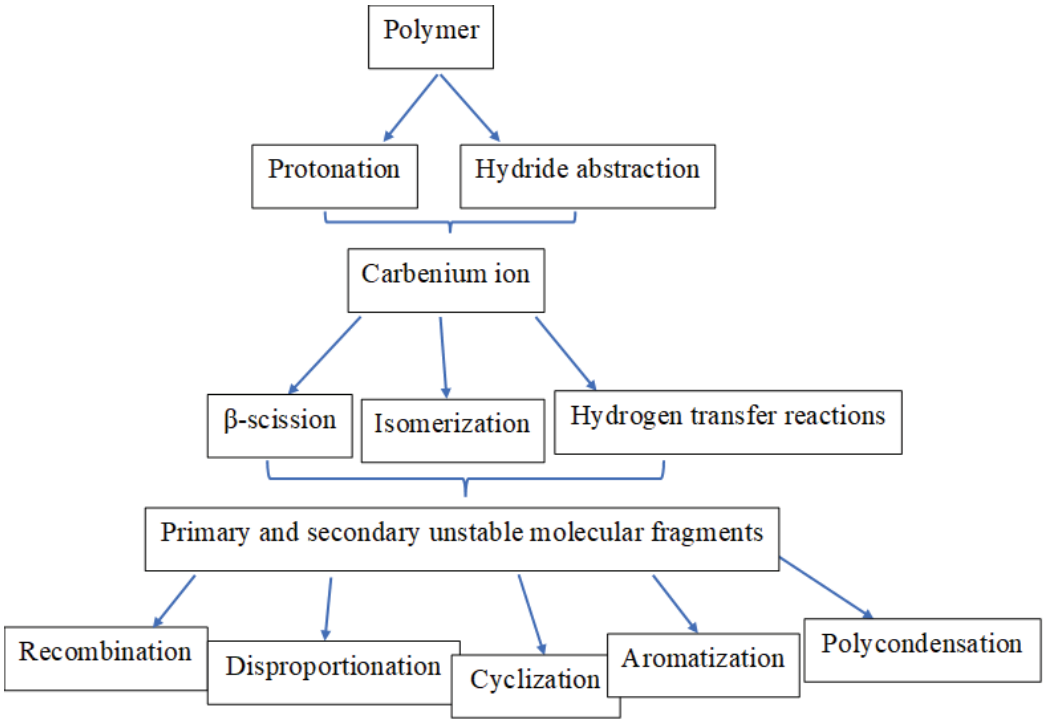


Figure 2. 1. The general catalytic polymer degradation mechanism.

Catalytic degradation of polyolefins can be started with random cracking or end-chain cracking. If random cracking occurs, firstly waxes are produced. Then they are cracked into gasoil ($C_{13}$-$C_{40}$), gasoline ($C_5$-$C_{12}$) and aromatic hydrocarbons ($C_6$-$C_9$) respectively. After hydrogen transfer to the aromatic hydrocarbons, there can be $C_3$-$C_5$ paraffins obtained. If the first step becomes end-chain cracking, $C_3$-$C_5$ olefins are produced directly. Then with oligomerization/cyclization reactions aromatic hydrocarbons can be produced. If hydrogen transfer performs for $C_3$-$C_5$ olefins, they can be converted to $C_3$-$C_5$ paraffins (D. P. Serrano 2012, Mehrdad Seifali Abbas-Abadi 2023).

The solid acid-catalyzed PE cracking mechanism's first step is initiating the reaction. Later β-scission or hydride-ion abstraction reactions can be performed. After that, a depropagation reaction occurs. As a result of chain cleavage and the sequential reaction of the polymers with carbonium ions, oligomers in the $C_{30}$–$C_{80}$ range are formed. With the β-scission reactions of these oligomers, gas and liquid products are obtained in the range of $C_{10}$–$C_{25}$. Then, isomerization and/or aromatization reactions are performed (A.G. Buekens 1998, Fan Zhang 2021).

# CHAPTER 3.

# MATERIALS AND METHODS

## 3.1. Feedstock

### 3.1.1. Feedstock preparation

Within the scope of the TÜBİTAK 119N302 project, household plastic waste (HPW), the packaging of these wastes, and some unclassified labels (i.e. labels on beverages, adhesive labels on detergent containers) were collected from certain regions in İzmir (Hatay, Gülbahçe, Urla) during the period of COVID-19 pandemic (January 2020 - September 2020). HPW was mainly composed of the packaging of food, cleaning agents, single-use products, and PET drinking bottles. Based on the resin identification codes (RIC) stated on the collected waste plastics, the major plastic types were determined as high-density polyethylene (HDPE) (softener and detergent containers, food packaging), low-density polyethylene (LDPE) (cleaning agents and food packaging), polypropylene (PP) (ice cream containers, packaging lids, chips packages), polystyrene (PS) (disposable cutlery, foam food containers), polyethylene terephthalate (PET) (beverage bottles, cleaning packaging), and others (i.e. PC) (food packaging). All collected plastics were separated according to their types and weighed according to the RIC symbols. Two separate classifications were made, with and without PET water drinking bottles. As indicated in Figure 3.1, the mass distribution of collected waste plastics was 30.0 wt.% PET (without water drinking bottles), 26.4 wt.% HDPE, 11.1 wt.% LDPE, 27.6 wt.% PP, 1.0 wt.% PS, 3.4 wt.% others (PC), 0.2 wt.% packaging, 0.4 wt.% unclassified and 0 wt.% PVC.

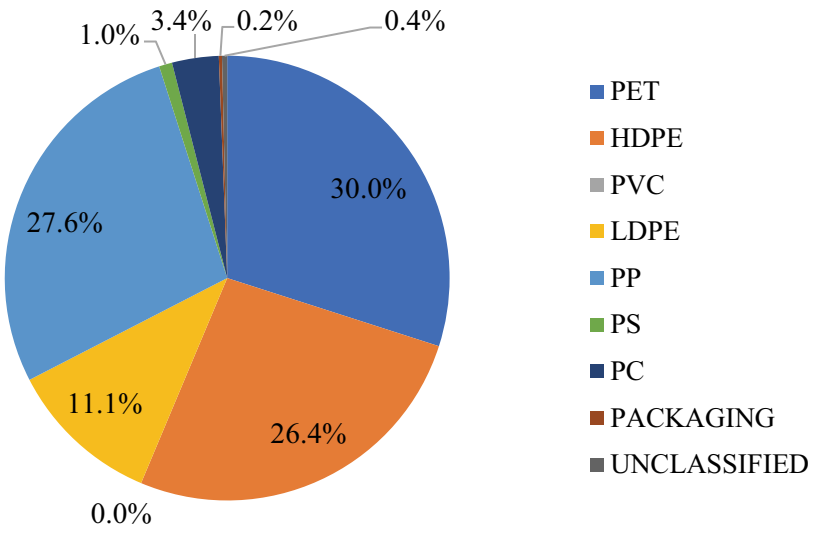


Figure 3. 1. Mass distribution of HPW collected in Izmir (excluding PET water drinking bottles).

For better comparability with the existing studies in the related literature, a dedicated polyolefin (PO) mixture is examined as a model feedstock in this thesis work. The mixture is composed of virgin (as received) HDPE, LDPE, and PP granules that were purchased from Pistonsan Plastik (Bornova, İzmir, Türkiye). The mass ratio of this mixture was determined based on the weight per cent distribution of collected waste plastics as shown in Figure 3.1. Waste plastic types other than HDPE, LDPE, and PP were excluded from the calculations and the shares of polyolefins in the mixture were determined as 40.5 wt.% for HDPE, 17.1 wt.% for LDPE and 42.4 wt.% for PP (Figure 3.2).

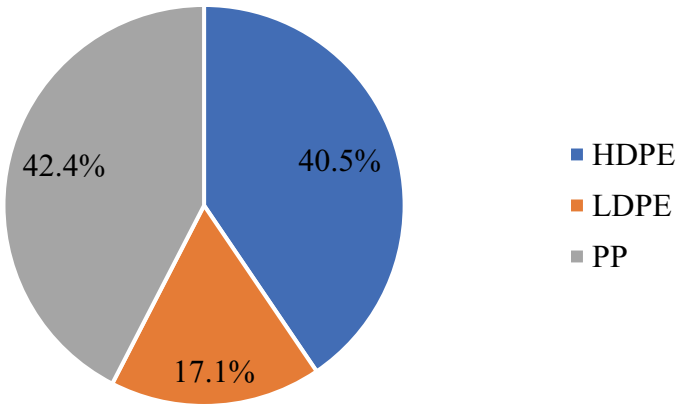


Figure 3. 2. Mass distribution in the feedstock prepared with virgin polyolefins.

### 3.1.2. Feedstock characterization

To investigate and compare the compatibility of polyolefin mixtures in the pyrolysis process, proximate and ultimate analyzes were performed. By using a Protherm 160/9 muffle furnace, moisture, volatile matter, and ash contents were determined for waste feedstocks according to the ASTM standards D 3173, D 3175, and D 3174, respectively. The amount of fixed carbon was calculated by difference. Table 4.1 represent the proximate analysis results of the waste PO plastics. The results of elemental (CHN/S) analysis were determined by a LecoTruSpec CHN Analyzer and shown in Table 4.2.

FTIR analysis of waste and virgin polyolefins was performed to determine the chemical bonds with ATR mode on a Bruker Alpha ECO-ATR instrument. Samples were scanned 64 times and the spectrum range and the wavelength resolution were 600-4000 $cm^{-1}$ and 4 $cm^{-1}$, respectively. Figure 4.1 (a, b) shows the wavelengths and related chemical bonds.

TGA analysis was performed to observe the mass loss in relation to an increase in temperature with PerkinElmer Simultaneous Thermal Analyzer STA6000. The PO samples were heated from 25 °C to 700 °C at a heating rate of 10 °C /min with an $N_2$ flow rate of 20 mL/min. Thermogravimetric results are illustrated in Figure 4.2. Then, DTG peaks were calculated as 469 °C, and 480 °C, respectively, to determine the maximum cracking temperature (Figure 4.3). Melting temperatures were determined using a DSC analysis by heating the samples from 25 °C to 350 °C at a 10 °C/min heating rate and 20 mL/min $N_2$ flow rate. In line with the findings in related literature studies, different melting peaks (Figure 4.4) that proved the presence of various polyolefins inside the waste PO mixture were found.

## 3.2. Catalyst

### 3.2.1. Selected catalyst types

Ammonium-based ZSM-5 (Si/Al=30, 50) in different silica-alumina mole ratios were purchased from Zeolyst International. The physicochemical properties of these acidic zeolite catalysts are illustrated in Table 3.1.

Table 3.1. Physicochemical characteristics of catalysts used in the study.

| Type | $SiO_2/Al_2O_3$ Mole Ratio | Nominal Cation Form | $Na_2O$, wt.% | Surface Area, $m^2/g$ |
|---|---|---|---|---|
| ZSM-5 | 30 | Ammonium | 0.05 | 405 |
| ZSM-5 | 50 | Ammonium | 0.05 | 425 |

### 3.2.2. Silica-Alumina production by single-step sol-gel method

A single-step sol-gel method was used to produce solid acid silica-alumina catalysts. In this study, catalysts were produced based on the Si/Al mole ratios of purchased zeolite catalysts. Two different silica-alumina catalysts (Si/Al=30 and Si/Al=50 mol ratios) and a ZSM-5 (Si/Al=50) supported silica-alumina (Si/Al=50) catalysts were produced, respectively. Si/Al mole ratios were converted to weight ratios. The physicochemical properties of produced catalysts can be seen in Table 3.2. To obtain alumina solution, aluminum isopropoxide (AIP) precursor, deionized (DI) water, and nitric acid ($HNO_3$), and to obtain silica solution, tetraethyl orthosilicate (TEOS) precursor, ethanol (EtOH), deionized (DI) water and hydrochloric acid (HCl) was used. The chemistry of this method includes hydrolysis (3.1) and condensation (3.2) reactions of metal precursors to obtain oxolation of metals:

$$-M-OR + H_2O \rightarrow -MOH + ROH \quad (3.1)$$

$$-M-OH + XO-M- \rightarrow -M-O-M- + XOH \quad (3.2)$$

Where M= metal; X = H or R (alkyl group) (KO 1997).

Table 3.2. Properties of silica-alumina catalysts produced via sol-gel method.

| Catalyst | $SiO_2/Al_2O_3$ Mol ratio | $SiO_2/Al_2O_3$ Weight ratio |
|---|---|---|
| Silica-alumina | 30 | 94.65%/5.35% |
| Silica-alumina | 50 | 96.72%/3.28% |
| ZSM-5 (Si/Al=50) supported silica-alumina | 50 | 96.72%/3.28% |

First, AIP and DI water were mixed at 900 rpm for 1 hour in a stirrer preheated to 85 °C. After 1 hour, $HNO_3$ was added to this solution, which was mixed for 1 hour under the same conditions. Meanwhile, in a separate stirrer, TEOS, EtOH, DI water, and HCl were added to each other, respectively, and heated from room temperature to 75 °C with 150 °C/min heating rate, mixed at 900 rpm for 1 hour. Later, the mixing processes were completed, the alumina solution was added to the silica solution, and the new mixture was stirred for 1 hour at 85 °C, 900 rpm to form a sol. After the sol was obtained, the mixing process was finished, and the borosilicate glass lid was opened for the gelation process at 70 °C. The transparent xerogel obtained after the gelation process lasted approximately 1 hour and was dried in an oven at 120 °C overnight. Calcination was applied, to silica-alumina catalysts obtained after drying, at 500 °C for 6 hours. Finally, the calcined catalysts were ground and sieved to 60 mesh, 250 µm (Figure 3.3).

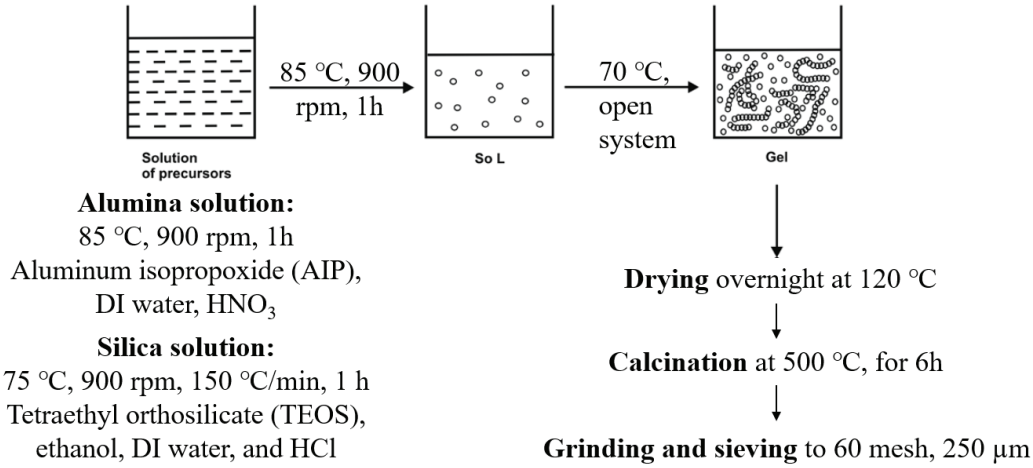


Figure 3.3. Schematic of single-step sol-gel method (Landau 2009).

While producing zeolite supported silica-alumina catalyst, unlike the procedure mentioned above, the alumina solution was added to the silica solution and mixed for 5 minutes at 85 °C, 900 rpm. Afterwards, the zeolite powder was added to the solution and stirred for 1 hour to obtain the new sol. The remaining steps were repeated precisely.

### 3.2.3. Catalyst characterization

$NH_3$-TPD analysis was used to identify the acidity and acidic strength of the catalysts. The catalysts were heated from room temperature to 500 °C with a 10 °C/min heating rate in the presence of helium (He) gas, waited at 500 °C for 30 minutes, and

cooled back to room temperature. Then He flow stopped for 1 hour, and $NH_3$ adsorption took place. After that, catalysts stayed at room temperature for 1 hour more, and the He was purged. Finally, the catalysts were reheated to 500 °C in the presence of He, and $NH_3$ desorption was performed. Total acidity (µmole $NH_3$/g of catalyst) was determined from the area under the peaks formed by the signals corresponding to time and temperature, and acidic strength was determined from the maximum desorption temperature. The total acidity and acidic strengths of silica-alumina (Si/Al=30), silica-alumina (Si/Al=50), ZSM-5 (Si/Al=50) supported silica-alumina (Si/Al=50), ZSM-5 (Si/Al=30), and ZSM-5 (Si/Al=50) catalysts are respectively as follows (Table 3.3).

Table 3. 3. Acidic properties of catalysts.

| **Catalyst type** | **Total acidity (µmole $NH_3$/g of catalyst)** | **Maximum desorption temperature (°C)** |
|---|---|---|
| Silica-alumina (Si/Al=30) | 402.72 | 479 |
| Silica-alumina (Si/Al=50) | 341.29 | 178 |
| ZSM-5 (Si/Al=50) supported silica-alumina | 349.92 | 172 |
| ZSM-5 (Si/Al=30) | 395.04 | 265 |
| ZSM-5 (Si/Al=50) | 371.89 | 250 |

FTIR analysis was used to determine the composition of fresh and spent catalysts with transmission mode on a Bruker Alpha instrument. The spectrum range was 400-4000 $cm^{-1}$. All samples and background were scanned 64 times. Wavelength resolutions were 4 $cm^{-1}$, and 2 $cm^{-1}$ respectively for fresh and spent catalysts. FTIR results of fresh catalysts can be seen in Figure 3.4 (Yihan Wang 2023, Dong Liu 2013, Seyed Amir Hossein Seyed Mousavi 2022). The 553.81 $cm^{-1}$ and 549.57 $cm^{-1}$ peaks illustrated in Figure 3 (b, c) proved the crystallinity of the catalysts. While the peak was not deep enough in ZSM-5 supported silica-alumina, the depth of the peak achieved by the ZSM-5 (50) catalyst was remarkable (Yihan Wang 2023).

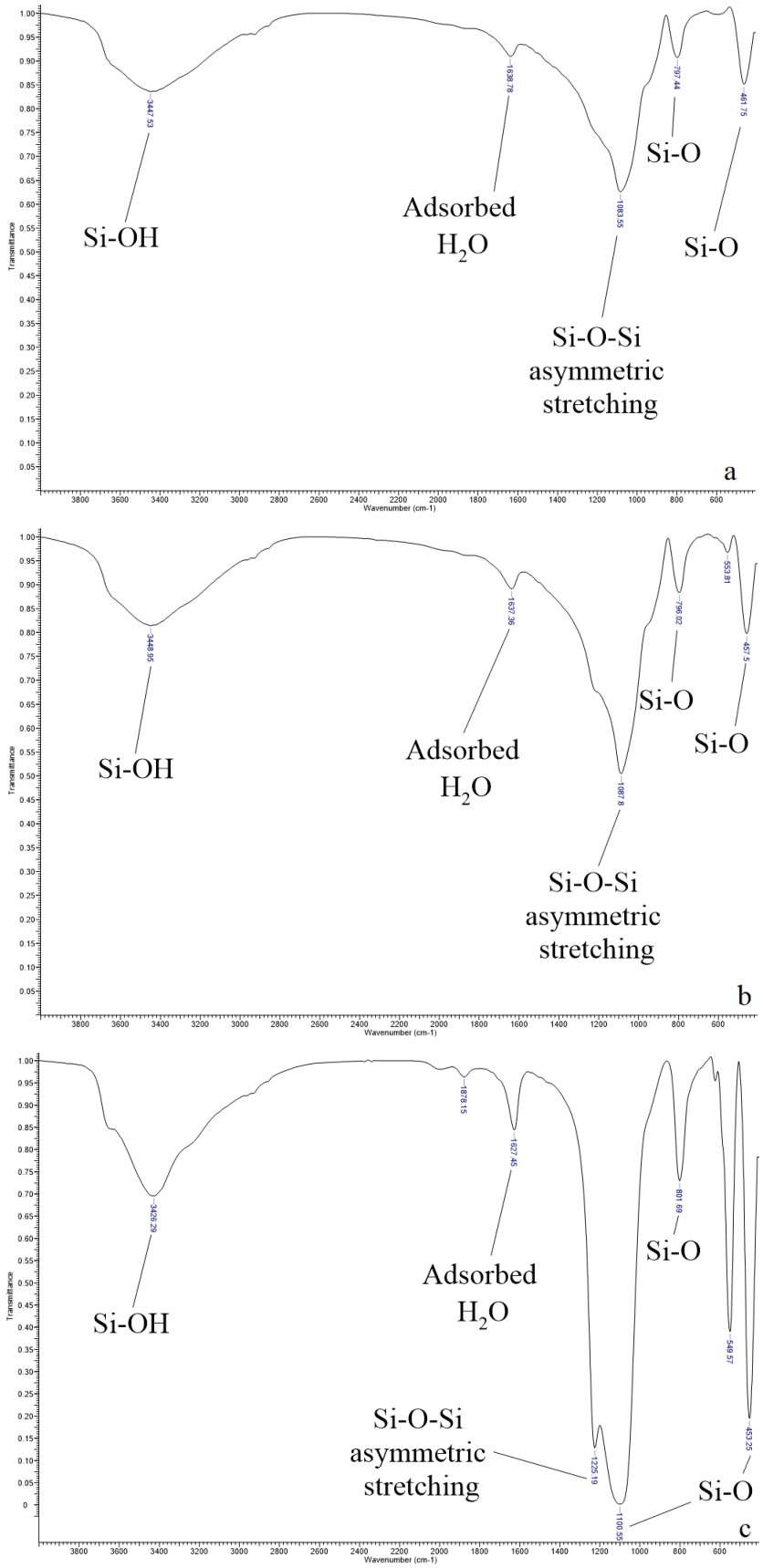


Figure 3.4. FTIR results of fresh a) Silica-alumina (Si/Al=50), b) ZSM-5 (Si/Al=50) supported silica-alumina, c) ZSM-5 (Si/Al=50) catalysts.

## 3.3. Experimental Set-Up and Process Parameters

In the pyrolysis experiments conducted for this thesis, only the feedstock consisting of virgin polyolefins (PO) were used. Operating conditions were determined as a result of the observed properties and comparisons in the feedstock characterization section (3.1.2.). Two different process modes were tested, namely continuous and batch. For continuous experiments, samples were prepared separately for each experiment as individually and as mixtures using the PO mixture distribution (40.5 wt.% for HDPE, 17.1 wt.% for LDPE and 42.4 wt.% for PP). For batch experiments, a fixed mass of feedstock sample was used with the mentioned PO distribution. The duration of the experiments was 1 hour for all the experiments.

### 3.3.1. Non-catalytic Pyrolysis

To determine the optimum conditions for thermal non-catalytic pyrolysis and to minimize the total number of experiments Taguchi's experimental design was used. For example, while the total number of experiments is 3^4=81 for a design with three levels and four control factors, this number can be reduced to nine experiments by applying the basic Taguchi L9 (3 4) orthogonal array.

#### 3.3.1.1. Continuously operated pyrolysis set-up

Figure 3.5 shows the schematic of the experimental set-up used for the pyrolysis of plastics. The primary experimental set-up included a mass flow controller (MFC), a thermal pyrolysis reactor, a mantle heater, a condenser, and a flask for liquid collection. For the PO mixture pyrolysis experiments, condensers were increased to two. Noncondensable gases were purged continuously from the system. While designing the experiment plan, the feeding period, the amount of feeding, the $N_2$ flow rate, and the cooling temperature of the chiller were determined as control factors. A table for Taguchi method-based experimentation was generated to examine the aforementioned factors individually at three different levels. The experiments were repeated at least twice. A model study was carried out with individual plastics (LDPE and PP). After understanding the behaviour of the plastic types, a virgin PO mixture was used with newly decided conditions. All experiments were carried out at a reaction temperature of 450 °C.

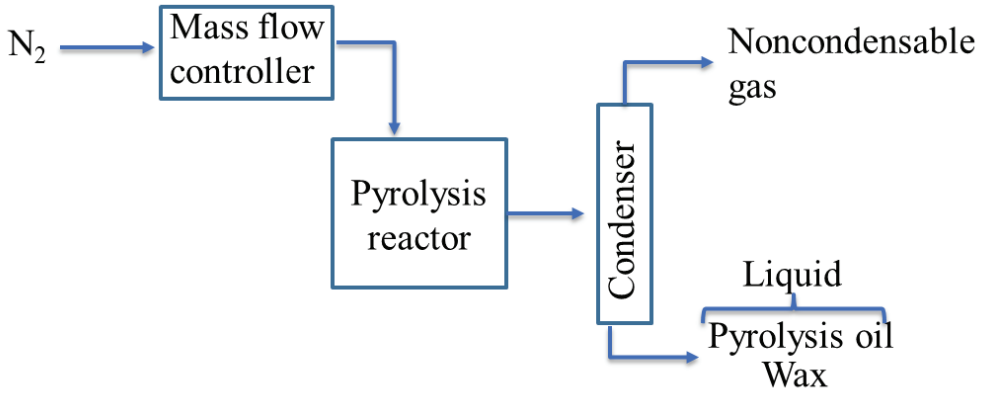


Figure 3.5. The schematic of the continuously operated pyrolysis set-up.

### 3.3.1.1.1. Experiments performed with low-density polyethylene (LDPE) as a feedstock

For the non-catalytic pyrolysis of low-density polyethylene (LDPE), the control factors were the $N_2$ flow rate, feeding period, plastic amount per feeding, and condensation temperature. Initially, it was determined how much the $N_2$ flow rate could be used in the system. Since the MFC can operate in the range of 500 to 5000 mL/min, the system's operation was observed by changing the flow rates. More than 1100 mL/min of $N_2$ flow rate caused operational problems due to a pressure increase in the system. Also, it was observed that pyrolysis vapours formed from LDPE could not be carried in the range of 500-800 mL/min. Therefore, three levels, 900, 1000, and 1100 mL/min, were determined as $N_2$ flow rates. Table 3.4 shows the process parameters for the non-catalytic pyrolysis of LDPE.

Table 3.4. The basic Taguchi L9 (3 4) orthogonal array for LDPE pyrolysis.

| Run | $N_2$ flow rate, mL/min | Feeding period, min | Plastic amount per feeding, g | Condensation temperature, °C |
|---|---|---|---|---|
| 1 | 900 | 10 | 10 | 0 |
| 2 | 900 | 15 | 20 | -5 |
| 3 | 900 | 20 | 30 | -10 |
| 4 | 1000 | 10 | 20 | -10 |
| 5 | 1000 | 15 | 30 | 0 |
| 6 | 1000 | 20 | 10 | -5 |
| 7 | 1100 | 10 | 30 | -5 |
| 8 | 1100 | 15 | 10 | -10 |
| 9 | 1100 | 20 | 20 | 0 |

### 3.3.1.1.2. Experiments performed with polypropylene (PP) as a feedstock

For the non-catalytic pyrolysis of polypropylene (PP), another experimental design was performed using the same control factors. Again, using the same methodology mentioned above for the LDPE pyrolysis, the $N_2$ flow rate range was determined as 800, 900, and 1000 mL/min. The new condensation temperatures were lowered, from 0 °C to -25 °C, to collect liquids more effectively. The feeding period and the amount of feedstock fed were kept the same as the previous in LDPE pyrolysis. All operation parameters are specified in Table 3.5.

Table 3.5. The basic Taguchi L9 (3 4) orthogonal array for PP.

| Run | $N_2$ flow rate, mL/min | Feeding period, min | Plastic amount per feeding, g | Condensation temperature, °C |
|---|---|---|---|---|
| 1 | 900 | 10 | 10 | 0 |
| 2 | 900 | 15 | 20 | -12.5 |
| 3 | 900 | 20 | 30 | -25 |
| 4 | 800 | 10 | 20 | -25 |
| 5 | 800 | 15 | 30 | 0 |
| 6 | 800 | 20 | 10 | -12.5 |
| 7 | 1000 | 10 | 30 | -12.5 |
| 8 | 1000 | 15 | 10 | -25 |
| 9 | 1000 | 20 | 20 | 0 |

### 3.3.1.1.3. Experiments performed with the polyolefin (PO) mixture as a feedstock

After the model tests for LDPE and PP were completed, control factors and levels were determined for the target feedstock (i.e. polyolefin mixture) used in this thesis. The feeding rate (g/min) was used as a new parameter. Three different feeding rates were selected (0.5 g/min, 1 g/min, and 1.5 g/min). The polyolefin (PO) feedstock was fed every 15 minutes for the operational ease of continuous feeding. Feeding amounts were selected as 7.5 g, 15 g, and 22.5 grams, respectively. $N_2$ flow rate was chosen as 900, 1000, and 1100 mL/min. The number of condensers has been increased to two, aiming for efficient liquid collection & separation. Tap water (ca. 15 °C) was used in the first condenser, and

an ethylene glycol-DI water mixture (chiller) was used in the second one at -25 °C. Table 3.6 shows the parameters used in nine experiments performed by using the PO mixture.

Table 3.6. Design of experiment for PO Mixture in the continuously operated experimental set-up.

| Run | $N_2$ flow rate, mL/min | Feeding rate, g/min |
|---|---|---|
| 1 | 900 | 0.5 |
| 2 | 900 | 1 |
| 3 | 900 | 1.5 |
| 4 | 1000 | 0.5 |
| 5 | 1000 | 1 |
| 6 | 1000 | 1.5 |
| 7 | 1100 | 0.5 |
| 8 | 1100 | 1 |
| 9 | 1100 | 1.5 |
| W | 1100 | 1.5 |

### 3.3.1.2. Pyrolysis set-up operating batch-wise

The bench-scale system made of glass and operating batch-wise consists of a nitrogen gas source, gas flow meter, gas meter, non-catalytic pyrolysis reactor, an ex-situ catalytic reactor, and a condenser (Figure 3.6). The pyrolysis liquid is collected into the flask, and the noncondensable gas is purged. In the non-catalytic pyrolysis experiments performed in this system, no catalyst is fed to the ex-situ reactor. Firstly, the condenser is cooled externally with the help of an ice accumulator (0 °C), but when it was observed that this cooling did not affect positively the condensation of the pyrolysis vapours, the liquid products continued to be collected under ambient conditions (without applying external cooling). In the experimental plan performed in this set-up (Table 3.7), the feeding amount was kept constant, and the effect of the $N_2$ flow rate (to provide a short residence time, <2 s, for fast pyrolysis) was examined. An optimum condition was determined based on the maximum liquid amount. All the experiments repeated at least duplicates.

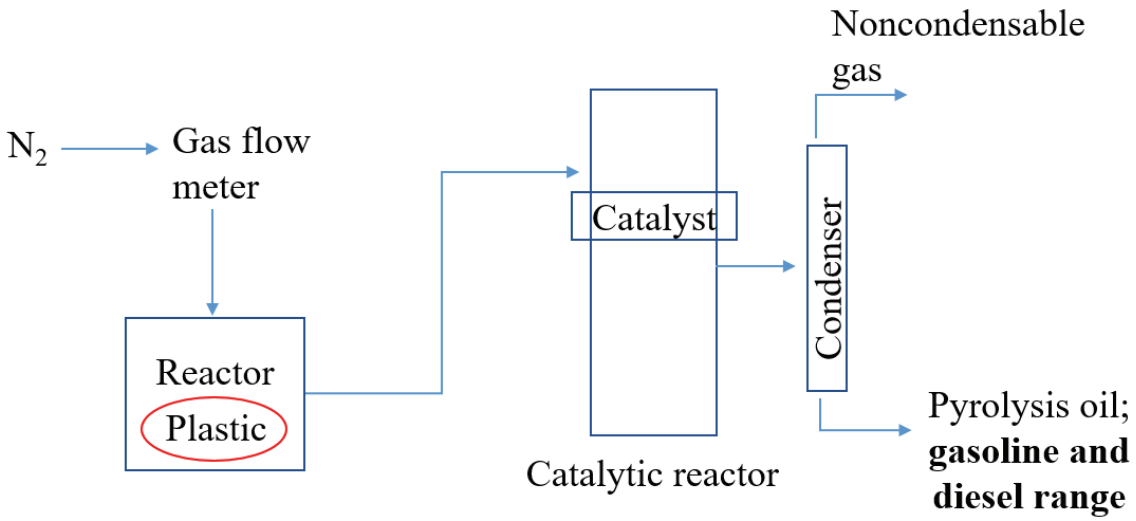


Figure 3.6. Experimental set-up for batch-wise operating pyrolysis.

Table 3.7. Experimental parameters for the pyrolysis of PO mixture performed in the set-up operating batch-wise.

| Run | $N_2$ flow rate, mL/min | Feedstock, g |
|---|---|---|
| T1 | 100 | 5 |
| T2 | 150 | 5 |
| T3 | 200 | 5 |

### 3.3.2. Catalytic Pyrolysis

Prior to each experiment, zeolites were calcined at 550 °C for 5 hours to obtain the hydrogen form, increase the acidity of the catalyst, and supply an efficient cracking of polyolefins.

#### 3.3.2.1. In-situ Catalytic Pyrolysis (CP) of LDPE

In the research conducted for the ISMO 2022 (Innovations-Sustainability-Modernity-Openness) Conference, liquid production was observed by in-situ catalytic pyrolysis of virgin LDPE. At first, as a result of the Taguchi experimental design prepared for the thermal pyrolysis of LDPE, the condition that providing a high liquid yield (77.7 wt.%) and producing the highest amount of wax was selected (Run 5 (1000 mL/min $N_2$ flow rate, 0 °C condensation temperature), Table 3.8). The effect of two different catalysts (ZSM-5 (Si/Al=30) and silica-alumina (Si/Al=30)) and four different catalyst-to-plastic ratios were investigated on the liquid amount and content. In this experimental set, the

continuously operated pyrolysis set-up (Figure 3.5) was used batch-wise. Catalysts and plastics were mixed and loaded into the reactor. The pyrolysis reactor was operated at 450 °C. For the catalytic pyrolysis in the presence of ZSM-5 (30), the catalyst-to-plastic ratios were determined as 1/100, 1/500, 1/1000, and 1/250 respectively. In-situ CP of silica-alumina catalyst was performed in the condition (1/250) where the abundant and fluid/nonviscous liquid was obtained. The pyrolysis products of these two catalysts were compared. The experimental conditions are given in Table 3.8.

Table 3.8. Catalyst types and catalyst-to-plastic ratios tested for the in situ catalytic pyrolysis (CP) of LDPE.

| Run | Catalyst type | Catalyst-to-plastic ratio |
|---|---|---|
| **5** | Non-catalytic | - |
| **5.1** | ZSM-5 (30) | 1/100 |
| **5.2** | ZSM-5 (30) | 1/500 |
| **5.3** | ZSM-5 (30) | 1/1000 |
| **5.4** | ZSM-5 (30) | 1/250 |
| **5.5** | Silica-alumina (30) | 1/250 |

### 3.3.2.2. Ex-situ Catalytic Pyrolysis (CP) of PO Mixture

While deciding on the ex-situ catalytic pyrolysis (ex-situ CP) conditions, the effect of catalyst mass and height on the experiment was examined, and a maximum of 1 cm high catalyst could be used to avoid situations such as gas blockage and/or pressure drop. In addition, residence time was determined by proportioning the volume of the catalyst in the fixed bed and the $N_2$ flow rate to perform fast pyrolysis (< 2 s). Equations (3.1), (3.2), and (3.3) illustrates the catalyst to plastic ratio, weight hourly space velocity, and residence time calculations respectively.

$$Catalyst\ to\ plastic\ ratio = \frac{mass_{catalyst}}{mass_{plastic}} \quad 3.1$$

$$WHSV\ (h^{-1}) = \frac{\frac{mass_{plastic}}{experiment\ time}}{mass_{catalyst}} = \frac{1}{Space\ time}(h) \quad 3.2$$

$$Residence\ time\ (s) = \frac{Volume_{catalyst}}{N_2\ flowrate} \quad 3.3$$

Table 3.9. Operation parameters for the ex-situ CP of PO mixture.

| Run | Catalyst type | Catalyst to plastic ratio | Space time, h | WHSV, $h^{-1}$ |
|---|---|---|---|---|
| 1 | ZSM-5 (50) | 1/500 | 0.002 | 500 |
| 2 | ZSM-5 (50) | 1/200 | 0.005 | 200 |
| 3 | Silica-alumina (50) | 1/500 | 0.002 | 500 |
| 4 | Silica-alumina (50) | 1/200 | 0.005 | 200 |
| 5 | Silica-alumina (50) via ZSM-5 (50) | 1/500 | 0.002 | 500 |
| 6 | Silica-alumina (50) via ZSM-5 (50) | 1/200 | 0.005 | 200 |

Experiments were carried out under the conditions in which the most liquid yield was obtained (Run T1, Table 3.7) in the experiments performed with the thermal pyrolysis set-up operating batch-wise (Figure 3.6). In each experiment, 100 mL/min $N_2$ gas was purged, and 5 grams of plastic was fed into the non-catalytic reactor. The fixed bed reactor was prepared by placing the catalysts, which were weighed according to the catalyst/plastic ratio in Table 3.9, with the glass wool. To reach target temperatures faster, both reactors were first heated to 80 °C. $N_2$ gas was fed for a certain period to provide an inert atmosphere. The ex-situ reactor was heated to 450 °C. Then the non-catalytic reactor started to heat up (up to 480 °C) and this was accepted as the t = 0 moment. At the end of each 1-hour experiment, liquid products were collected into the flask. The experimental plan established with three different catalysts and two different weight hourly space velocities (WHSV, $h^{-1}$) is given in Table 3.9.

## 3.4. Products

### 3.4.1. Product Distribution

After the experiments, the masses of the pyrolysis liquid (in the flask) and residue (unconverted plastics/heavy wax/ash remaining in the reactor) were determined by weighing in a precision balance. No solid product was formed in the thermal experiments.

Coke formation was observed in catalytic experiments. No residue was formed in experiments performed with a ZSM-5 catalyst. For thermal experiments, liquid, and residue (if any) were collected after weighing, and the amounts of gas were calculated by difference.

The equation below illustrates the mass balance calculation of continuous thermal pyrolysis products of LDPE, PP and PO Mixture:

$$m_{feedstock} = m_{liquid} + m_{gas} + m_{residue} \quad 3.4$$

The mass balance calculation of the batch thermal pyrolysis products of the PO Mixture:

$$m_{feedstock} = m_{liquid} + m_{gas} + m_{residue} \quad 3.5$$

The mass balance calculation of LDPE's batch-operated in situ catalytic pyrolysis products:

$$m_{feedstock} = m_{liquid} + m_{gas} + m_{solid\,(coke)} + m_{residue} \quad 3.6$$

The mass balance calculation of PO Mixture's ex situ catalytic pyrolysis products:

$$m_{feedstock} = m_{liquid} + m_{gas} + m_{solid\,(coke)} + m_{residue} \quad 3.7$$

The yields of products (wt.%) were calculated by the ratio of the mass of the products to the total mass of feedstock individually.

$$\frac{m_{liquid}}{m_{feedstock}} x\ 100\% = liquid\ yield\ (wt.\%) \quad 3.8$$

$$\frac{m_{gas}}{m_{feedstock}} x\ 100\% = gas\ yield\ (wt.\%) \quad 3.9$$

$$\frac{m_{solid}}{m_{feedstock}} x\ 100\% = solid\ (coke)\ yield\ (wt.\%) \quad 3.10$$

$$\frac{m_{residue}}{m_{feedstock}} x\ 100\% = residue\ yield\ (wt.\%) \quad 3.11$$

The conversion was calculated by dividing the targeted products' total masses by the feedstock amount.

$$\frac{m_{liquid}+m_{gas}}{m_{PO\ Mixture}} x\ 100\% = \%\ conversion \quad 3.12$$

## 3.4.2. Product Characterization

GC-MS analysis was performed by HP-5MS capillary column to investigate the content of liquid ($C_5$-$C_{40+}$) products. The program started at 40 ℃ and held for 2 minutes. Then liquid hydrocarbons (HCs) were heated to 200 ℃ with a 3 ℃/min heating rate for 55 minutes. In the second ramp, with a 5 ℃/min heating rate HCs were heated to 320 ℃ and held for 10 minutes. Thanks to the identical peaks observed and using libraries, chemical formulas, and carbon number distribution could be determined.

FTIR analysis was used to determine the chemical bonding of compounds in liquid products with ATR mode on a Bruker Alpha ECO-ATR instrument. The spectrum range

was 600-4000 $cm^{-1}$, wavelength resolution was 4 $cm^{-1}$ and both the liquid sample and background were scanned 64 times.

# CHAPTER 4

# RESULTS AND DISCUSSIONS

## 4.1. Feedstock Characterization

By the proximate analysis, of how much volatile matter is converted from plastics, it was possible to get an idea about the amount of fuel that can be obtained. Before the pyrolysis application, the presence of nitrogen, sulfur and oxygen in the raw material content was determined. This information helped to predict whether the raw material needs pretreatment and the quality of the fuel to be produced. In addition, the amount of oxygen detected in the content of plastic packaging materials showed that they were not produced completely pure. Proximate and elemental analysis results of waste polyolefins are given in Table 4.1 and Table 4.2 below.

Table 4.1. The results of proximate analysis of waste polyolefins.

| | **Moisture (wt.%)** | **Volatile Matter (wt.%)** | **Ash (wt.%)** | **Fixed Carbon (wt.%)*** |
|---|---|---|---|---|
| HDPE | 0,33 ± 0,03 | 97,07 ± 1,26 | 0,96 ± 0,10 | 1,63 ± 1,15 |
| LDPE | 1,33 ± 1,39 | 93,27 ± 1,49 | 1,74 ± 0,05 | 3,65 ± 0,17 |
| PP | 0,38 ± 0,02 | 94,75 ± 2,11 | 2,30 ± 0,20 | 2,58 ± 2,19 |

*By difference

Table 4. 2. The results of ultimate analysis of waste polyolefins.

| | **C (%)** | **H (%)** | **N (%)** | **S (%)** | **O (%)*** |
|---|---|---|---|---|---|
| HDPE | 85.08±0.44 | 14.41±0.02 | 0.00 | 0.00 | 0.51±0.43 |
| LDPE | 81.61±0.35 | 13.22±0.26 | 0.00 | 0.00 | 5.17±0.53 |
| PP | 80.93±0.23 | 13.47±0.2 | 0.00 | 0.00 | 5.6±0.3 |

*By difference

FTIR technique was also applied for the characterization of the raw material. Figure 4.1 shows the included chemical groups of waste and virgin polyolefin mixtures. Except for the C=C bond seen in the virgin PO mixture, it was observed that the other peaks were common with each other.

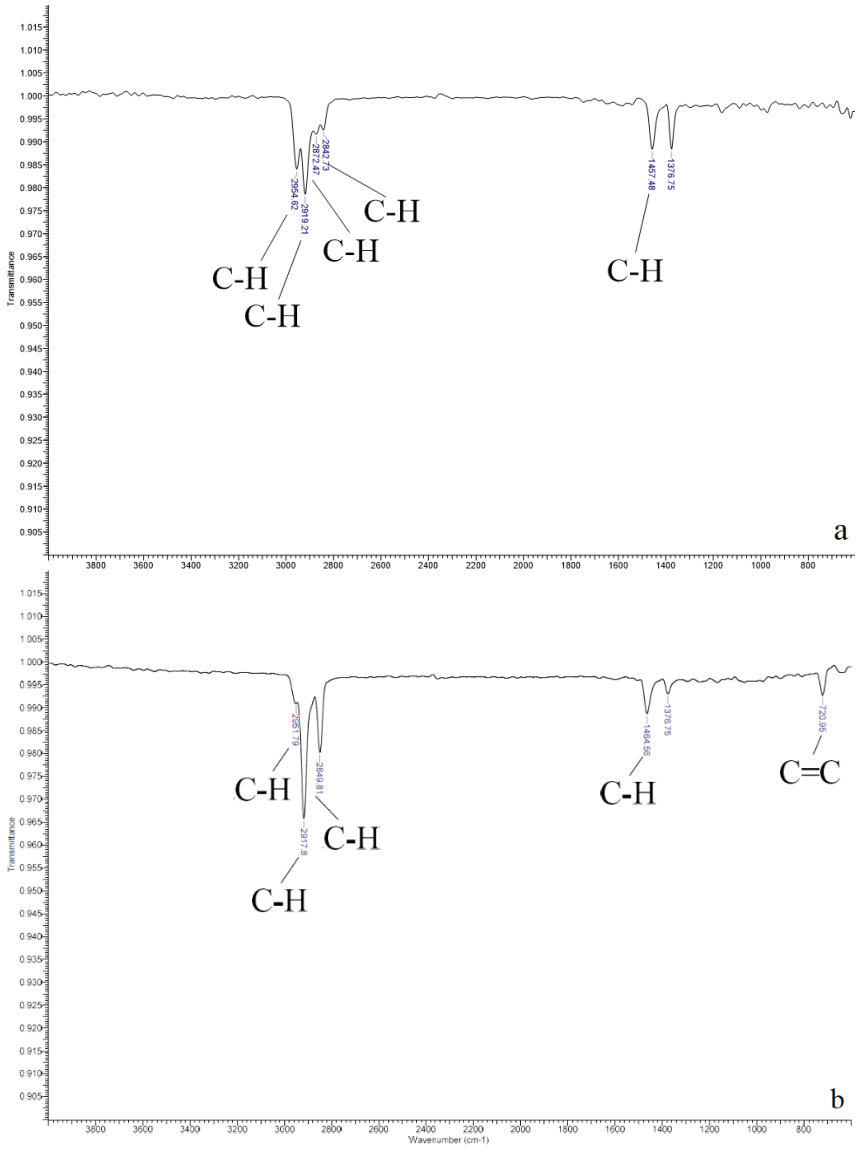


Figure 4. 1. FTIR results of a) waste PO mixture, b) virgin PO mixture.

TGA-DTG analyses were used to predict the thermal behaviour of polyolefins when pyrolysed individually and as a mixture. Virgin PP, virgin HDPE, virgin LDPE, and virgin PO mixture started to crack thermally at 240 ℃, 336 ℃, 324 ℃, and 311 ℃, respectively (Figure 4.2).

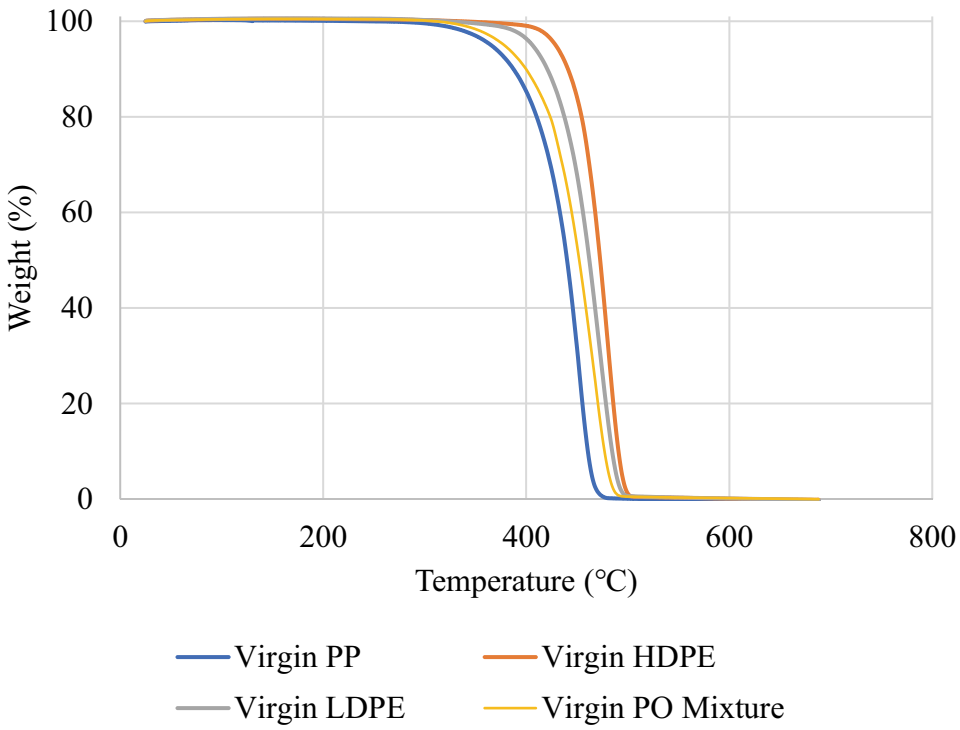


Figure 4. 2. Thermogravimetric analysis results of virgin polyolefins.

The temperatures at which maximum cracking occurs are 453 °C, 480 °C, 474 °C and 469 °C for virgin PP, HDPE, LDPE, and PO mixture, respectively (Figure 4.3). It was determined that the maximum degradation temperature of the polyolefin mixture, creating a synergistic effect, decreased compared to polyethylene and increased compared to polypropylene.

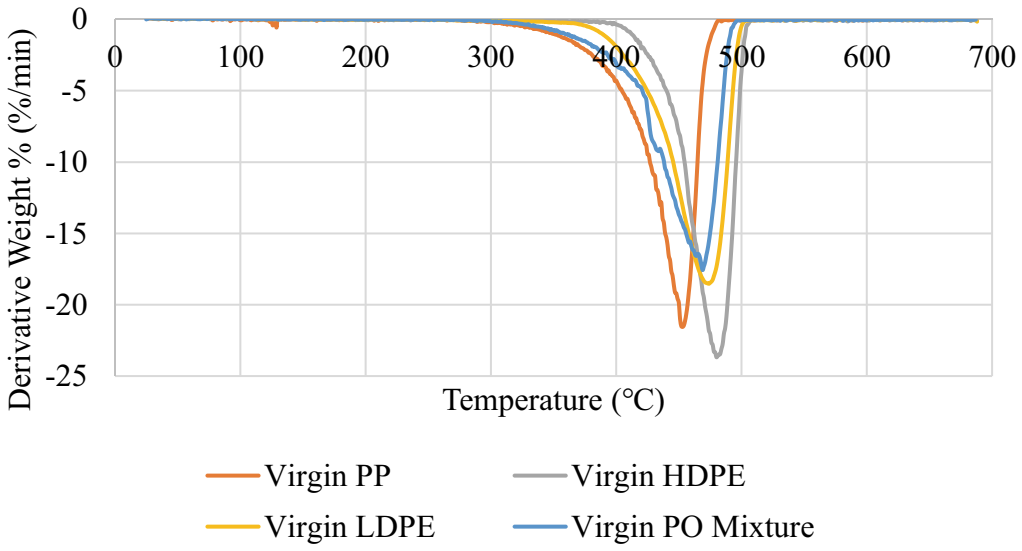


Figure 4. 3. DTG results of virgin polyolefins.

Melting points of polyolefins were determined by DSC analysis. Virgin PP, HDPE, and LDPE started to melt at 164 ℃, 131 ℃ and 108 ℃ (Figure 4.4). The fact that the prepared PO mixture has the same melting peaks made it possible to understand that the mixture was prepared homogeneously.

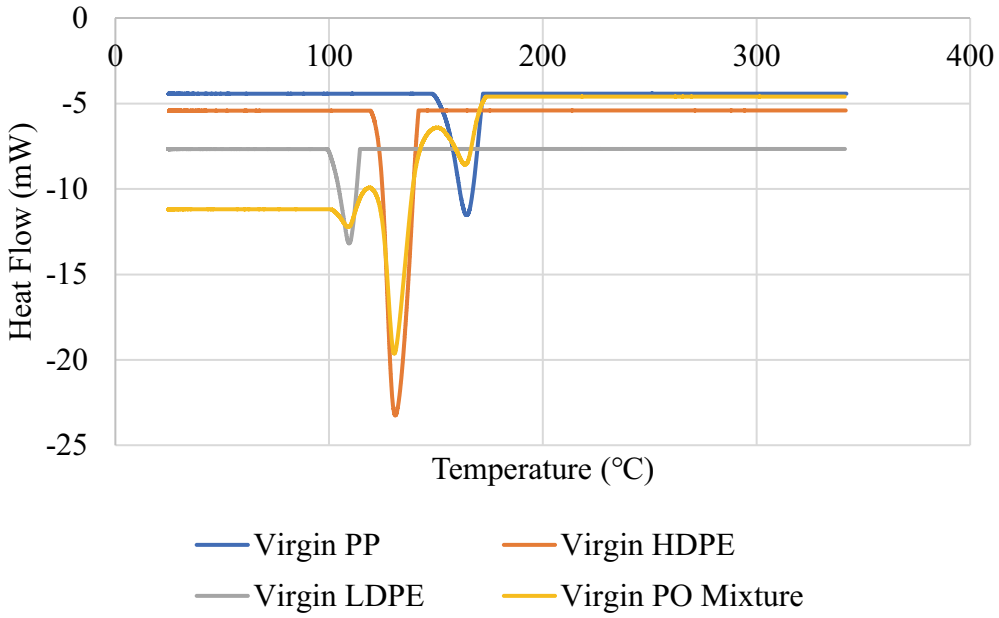


Figure 4. 4. Melting points defined by DSC of virgin polyolefins.

## 4.2. Non-catalytic Pyrolysis

### 4.2.1. Continuously operated pyrolysis set-up

#### 4.2.1.1. Experiments performed with low-density polyethylene (LDPE) as a feedstock

In non-catalytic test experiments of LDPE, the effect of process parameters such as $N_2$ flow rate, feeding period, plastic amount per feeding, and condensation temperature on product distribution was investigated. As learned from the literature, large amounts of wax formation were expected in LDPE pyrolysis. First, the experiments that provided the highest conversion and produced the most liquid were determined (Table 4.3). The reason for this was to obtain the pyrolysis oil with the highest efficiency.

Table 4.3. Product yields and conversion of LDPE pyrolysis.

| | Yield, wt.% | | | |
|---|---|---|---|---|
| **Run** | **Liquid** | **Gas** | **Residue** | **Conversion, wt.%** |
| **1** | 53.11 | 4.93 | 41.96 | 58.04 |
| **2** | 91.51 | 5.25 | 3.25 | 96.75 |
| **3** | 64.38 | 25.18 | 15.67 | 89.57 |
| **4** | 55.01 | 23.60 | 21.39 | 78.61 |
| **5** | 77.70 | 20.55 | 1.75 | 98.25 |
| **6** | 58.25 | 35.10 | 6.66 | 93.34 |
| **7** | 70.77 | 16.13 | 13.10 | 86.90 |
| **8** | 63.42 | 35.33 | 1.25 | 98.75 |
| **9** | 73.72 | 25.78 | 0.50 | 99.50 |

The effect of 900 mL/min $N_2$ flow rate was investigated in the first three experiments in the 9 experiments Taguchi planning prepared for the thermal pyrolysis of LDPE plastic. In Run 1, a total of 60 grams of virgin LDPE was pyrolyzed by adding 10 grams of plastic every 10 minutes. Approximately 58 wt.% conversion was achieved and 53 wt.% liquid was produced. Run 2 carried out a total of 80 grams of virgin LDPE pyrolysis by feeding 20 grams of plastic every 15 minutes. While 96.75 wt.% conversion was achieved, 91.51 wt.% liquid was produced. In Run 3, 30 grams were fed into the system every 20 minutes, i.e. 90 grams in total. By providing 89.57 wt.% conversion, 64.38 wt.% liquid product was obtained. The condition that was primarily compared to these three experiments was the feeding rate (plastic amount/feeding period). From Run 1 to Run 3, the feeding rate increased from 1 g/min to 1.5 g/min. While the positive effect of the increase in feeding rate was observed when switching from Run 1 to Run 2, the same effect was not observed from Run 2 to Run 3. In addition to all these, the condensation temperature was reduced respectively in these 3 experiments, and it was aimed to collect liquid products more effectively. When the condensation temperature decreased from 0 °C to -5 °C, the positive effect observed in the amount of liquid was not observed when it decreased from -5 °C to -10 °C.

The $N_2$ flow rate used in the Run 4-6 interval was increased to 1000 mL/min. In Run 4, a total of 120 grams of LDPE was pyrolyzed by adding 20 grams of plastic continuously every 10 minutes. 78.6 wt.% conversion was achieved and approximately 55 wt.% liquid was produced. In Run 5, a total of 120 grams of virgin LDPE pyrolysis was carried out by feeding 30 grams of plastic every 15 minutes. While 98.25 wt.% conversion was achieved, 77.7 wt.% liquid was produced. The $N_2$ flow rate as well as the

feeding rate, 2 g/min, was common in these two experiments. The feeding rate was the same in both experiments, but the liquid efficiency and conversion also differed markedly. This situation clearly emphasized the importance of feeding period and amount. The effect of feeding every 15 minutes and every 10 minutes on the residue yield and thus on conversion gave an idea for further experiments (i.e. Section 3.3.1.1 PO Mixture as a feedstock). In Run 6, 10 grams of LDPE, i.e. 30 grams in total, was fed to the system every 20 minutes. 93.34 wt.% conversion was achieved, but the liquid yield could not exceed 58.25 wt.%. The interpretation that can be made here was that the pyrolysis vapor, which consists of plastic fed in small amounts and at long intervals, stays in the reactor for a long time and causes secondary cracking, thereby increasing the gas amount. In addition, the fact that the condensation temperatures used as -10 °C, 0 °C, and -5 °C, had no direct proportional effect on the amount of liquid product.

The $N_2$ flow rate used for Run 7-9 was 1100 mL/min. The conditions for Run 7 were 30 grams of LDPE feeding to the reactor every 10 minutes. Thus, the highest total amount of plastic between these 9 experiments was determined as 180 grams for Run 7. As a result of this experiment, 86.9 wt.% conversion was provided and 70.77 wt.% liquid product was obtained. In Run 8, the plastics of 10 grams were pyrolyzed in every 15 minutes and even though 98.75 wt.% conversion was reached, the liquid yield was 63.42 wt.%. In Run 8, as in Run 6, a small amount of plastic stayed for a long time in the reactor, which had a negative effect on the production of liquid and a positive contribution to the amount of noncondensable gas. It can also be said that the $N_2$ flow rate, which was compared for these two similar experiments, better purged the pyrolysis vapours and prevented the secondary reactions. Finally, in the 9th experiment, when the effect of 20 grams of plastic feeding every 20 minutes was examined, a pyrolysis fluid of 73.72 wt.% and 99.5 wt.% conversion was achieved. In addition, this experiment was compared with Run 1, which was common in the feeding rate condition, an increase of $N_2$ flow rate from 900 mL/min to 1100 mL/min promoted the liquid production in terms of sweeping the pyrolysis vapours and inhibiting secondary cracking.

Conversions of Runs 5, 8, and 9 are 98.25 wt.%, 98.75 wt.%, and 99.5% wt.%, respectively. Among these three high-conversion experiments, the highest liquid yield was 77.7 wt.% by the Run 5 experiment. It was also observed that the formation of 20.55 wt.% gas and 1.75 wt.% residue. By Run 8, while 63.42 wt.% liquid was produced, 35.33 wt.% gas and 1.25 wt.% residue were generated. In the conditions of Run 9, 73.72 wt.%

liquid, 25.78 wt.% gas and 0.5 wt.% residue were obtained. In addition to these, 91.5 wt.% liquid (no wax) obtained as a result of the Run 2 experiments was also remarkable.

However, as a result of the comparison of the mentioned four experiments, the Run 5 test (1000 mL/min $N_2$ flow rate, 2 g/min feeding rate, 0 °C condensation temperature), in which all of the pyrolysis liquid produced was collected as wax, was chosen as a reference to be used in the catalytic pyrolysis experiments to be applied in the next sections (4.3.1.).

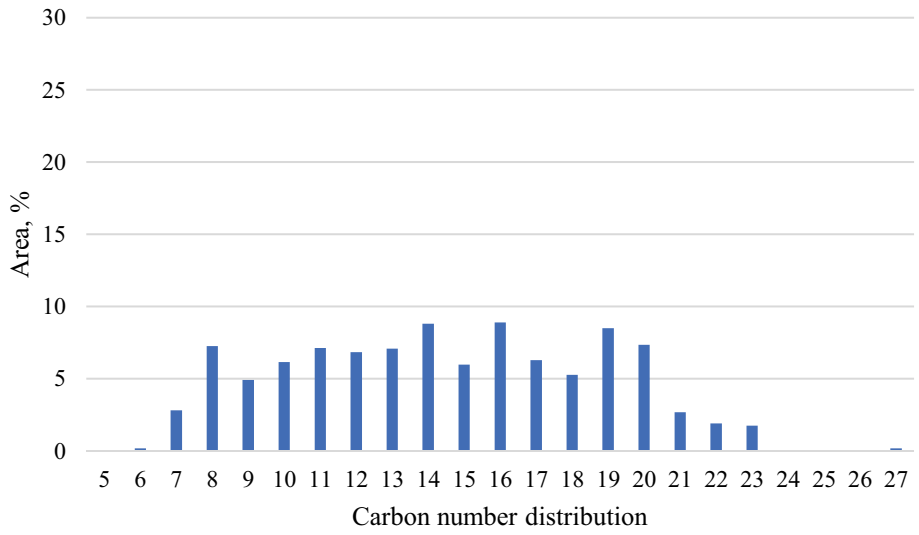


Figure 4. 5. Carbon number distribution of the liquid product of Run 5.

In Figure 4.5, the carbon number distribution of the waxy liquid produced with Run 5 is indicated. As stated in the literature hydrocarbon liquids are divided into $C_5$-$C_{12}$ as gasoline, $C_{13}$-$C_{20}$ as diesel, and $C_{21+}$ as wax. So that the produced liquid was divided into 29.67% gasoline, 57.46% diesel and 12.87% wax range hydrocarbons (Figure 4.6). Besides, no benzene, toluene, and/or xylene aromatics were detected.

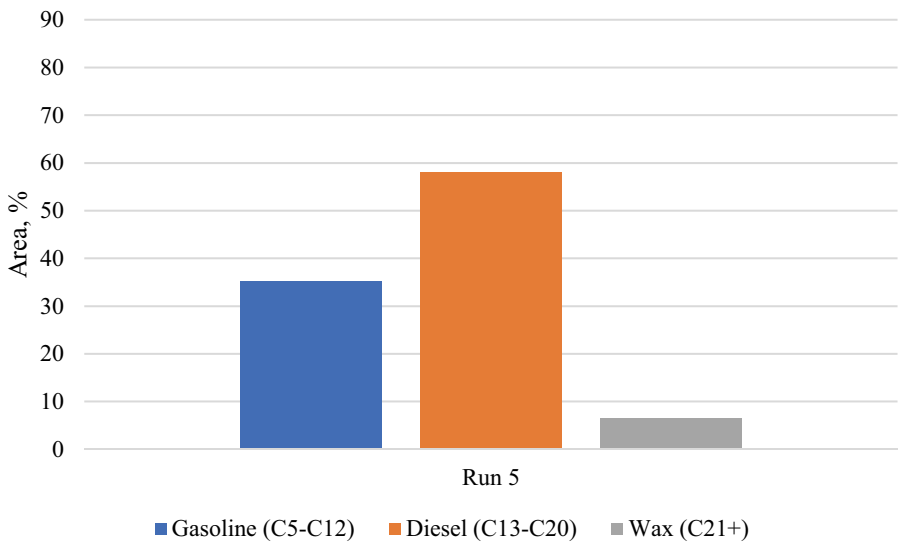


Figure 4. 6. The liquid product distribution of Run 5 according to hydrocarbon range.

### 4.2.1.2. Experiments performed with polypropylene (PP) as a feedstock

After the test experiments with virgin LDPE plastic, thermal pyrolysis test experiments were carried out for another polyolefin type, polypropylene (PP). The same operation parameters in the LDPE test experiments were examined, but according to the process operation (due to the pressure problems) $N_2$ flow rate was used as 800, 900, and 1000 mL/min. The feeding period and amount were applied as same as in the Taguchi test table of LDPE. The condensation temperature was changed to 0 °C, -12.5 °C, and -25 °C based on previous experimental observations and due to the problems encountered at the beginning of the PP test experiments. Related results of PP pyrolysis experiments are shown in Table 4.4.

Table 4. 4. Product yields and conversion of PP pyrolysis.

| Run | Liquid, wt.% | Gas, wt.% | Residue, wt.% | Conversion, wt.% |
|---|---|---|---|---|
| **1** | 67.33 | 24.52 | 8.15 | 91.85 |
| **2** | 72.04 | 22.72 | 5.24 | 94.76 |
| **3** | 75.03 | 21.94 | 3.03 | 96.97 |
| **4** | 63.22 | 15.21 | 21.57 | 78.43 |
| **5** | 62.21 | 17.97 | 19.82 | 80.18 |
| **6** | 69.16 | 30.50 | 0.33 | 99.67 |
| **7** | 58.75 | 17.99 | 23.27 | 76.73 |
| **8** | 73.60 | 24.15 | 2.25 | 97.75 |
| **9** | 78.41 | 20.59 | 1.00 | 99.00 |

In the first three experiments, thermal pyrolysis of PP plastic was carried out with an $N_2$ flow rate of 900 mL/min. A total of 60, 80, and 90 grams of PP were pyrolyzed at a feeding rate of 1 g/min in Run 1, 1.33 g/min in Run 2, and 1.5 g/min in Run 3. The variable conditions were the increase in feeding rate (1 g/min to 1.5 g/min) and a decrease in condensation temperature (0 °C to -25 °C). Run 1 through Run 3 achieved 91.85 wt.%, 94.76 wt.%, and 96.97 wt.% conversions, respectively. While the amount of gas produced was close to each other, it was observed that the amount of residue decreased as the feeding rate increased. Thus, the amount of liquid increased to 67.33 wt.%, 72.04 wt.%, and 75.03 wt.%, respectively. Based on these results, the amount of plastic fed and the length of time spent in the reactor should be carefully adjusted.

For Run 4-6 range PP polyolefins were pyrolyzed with 800 mL/min $N_2$ flow rate. Run 4 was fed 20 grams of plastic every 10 minutes. In Run 5, 30 grams of plastic was fed every 15 minutes. Except for the $N_2$ flow rate, the common point in these two experiments was a feeding rate of 2 g/min. With 78.43 wt.% and 80.18 wt.% conversions, 63.22 wt.% and 62.21 wt.% liquid products were obtained, respectively. It was remarkable that the liquid, gas and residue amounts were very close to each other. Although Run 4 produced more residue, it was able to collect more liquid. For both experiments, the amount of residue should be reduced, and it should be ensured that it contributes to the liquid and gas product. The reason for all this may be that the $N_2$ flow rate, which is reduced to 800 mL/min, cannot carry the pyrolysis vapour well enough and the increase in feeding rate does not allow enough cracking time. In the Run 6 experiment, 10 grams of PP was fed at 20-minute intervals and the feeding rate was reduced to 0.5 g/min. Conversion reached 99.67 wt.%, with the combination of decreased $N_2$ flow rate and feeding rate. 69.16 wt.% liquid and 30.5 wt.% gas were produced. The conclusion to be drawn from here was to see the effect of $N_2$ flow rate and plastic feeding with each other. After the $N_2$ flow rate decreased to 800 mL/min, when the increased feeding rate bring unconverted plastic with it, decreased flow rate was encountered with almost all recycled plastic and liquid products produced in more than two other experiments.

1000 mL/min $N_2$ flow rate was used in Run 7-9 experiments. In the experiment Run 7, 30 grams of plastic was pyrolyzed every 10 minutes. 76.73 wt.% conversion and 58.75 wt.% fluid production were achieved. The reason why conversion decreased was the increasing feeding rate and $N_2$ flow rate at the same time. Increasing the feeding rate to 3 g/min resulted in short feeding periods for relatively large amounts of plastic and became insufficient for thermal cracking. In addition, since the pyrolysis vapours

produced in the reactor were rapidly purged into the condenser, they could not crack sufficiently and the amount of liquid product decreased. In Run 8, 10 grams of PP was fed every 15 minutes. Unlike Run 7, the plastics had time to crack and resulted in a conversion of 97.75 wt.%. While the amount of gas increased to 24.15 wt.%, 73.6 wt.% liquid was obtained. For Run 9, applying a 1 g/min feeding rate 20 grams of PP was pyrolyzed at 20 minutes intervals. When the Run 1 and Run 9 experiments were compared over the $N_2$ flow rate which increased from 900 mL/min to 1000 mL/min, in constancy with the feeding rate and 0 ℃ condensation temperature, the residue and noncondensable gas were visibly decreased. These resulted in 99.0 wt.% conversions and the highest liquid yield of 78.41 wt.% (among all experiments). In terms of the $N_2$ flow rate increase in these two experiments, it can be said that better transport and condensation of pyrolysis vapours were ensured. At the same time, the amount of gas was higher due to the secondary cracking reactions that took place during the time spent in the reactor by the pyrolysis vapours formed from Run 1. However, pyrolysis vapour obtained from 20 grams of plastic fed at 20-minute intervals made a positive contribution to the liquid yield with the support of the $N_2$ flow rate increase, and gas product yield was significantly decreased.

In these new test experiments, the goal was again to find the experiment that produced the highest amount of liquid. Generally, conversions were higher than the pyrolysis of LDPE plastic. In addition, the resulting residue had a heavy wax/fuel appearance for LDPE, while PP formed unconverted plastic and ash as a residue. Runs 6, 8, and 9 yielded 99.67 wt.%, 97.75 wt.%, and 99.0 wt.% conversions, respectively. 69.16 wt.% liquid, 30.5 wt.% gas and 0.33 wt.% residue were obtained under the conditions of Run 6. With Run 7, while 73.6 wt.% liquid and 24.15 wt.% gas were collected, 2.25 wt.% residue was obtained. Moreover, when the Run 9 experiment was investigated, 78.41 wt.% liquid (the highest among all experiments, and completely in waxy form), 20.59 wt.% gas and 1.0 wt.% residue were observed. Thus, the Run 9 (1000 mL/min $N_2$ flow rate, 1 g/min feeding rate, 0 ℃ condensation temperature) test experiment was determined as the optimum condition.

The only test experiment in which two different polyolefins PP and LDPE were common in all conditions was Run 1 (900 mL/min $N_2$ flow rate, 10 min feeding period, 10 grams feeding amount, 0 ℃ condensation temperature). LDPE achieved 58.04 wt.% conversion under these conditions, while PP achieved 91.85 wt.% conversion. Apparently, 900 mL/min $N_2$ flow rate for 1 g/min feeding rate works more efficiently for

PP, but it is insufficient for LDPE. Another condition compared was Run 5 (15 min feeding period, 30 grams feeding amount, 0 °C condensation temperature) of LDPE and PP. For Run 5, the varying condition other than the plastic type was a decrease in the $N_2$ flow rate from 1000 mL/min to 800 mL/min. In these experiments using a 2 g/min feeding rate, 98.25 wt.% conversion was obtained from LDPE pyrolysis, while 80.18 wt.% conversion was obtained as a result of PP pyrolysis. This was because the 800 mL/min $N_2$ flow rate was insufficient for a 2 g/min PP feeding rate. In addition, when these two plastics were compared for Run 9 (20 min feeding period, 20 grams feeding amount, 0 °C condensation temperature), which was chosen as the optimum condition for PP, PP and LDPE successfully achieved 99.0 wt.% and 99.5 wt.% conversions, respectively. For Run 9, in addition to the plastic change, two different $N_2$ flow rates such as 1000 mL/min and 1100 mL/min were used. Even the conditions of Run 1 and Run 9 are common in terms of a feeding rate of 1 g/min. And it was clear that increasing the $N_2$ flow rate for both plastics, changing the feeding amount and the period to 20 grams of plastic every 20 minutes had a positive effect, resulting in the highest conversions among all compared conditions. Also, it was observed that the 0 °C condensation temperature was enough to collect liquid products for both the LDPE and PP pyrolysis.

#### 4.2.1.3. Experiments performed with a polyolefin (PO) mixture as a feedstock

After the test experiments of individual plastics, the thermal pyrolysis of the virgin polyolefin mixture was investigated at the ratio determined at the beginning of this thesis research (Figure 3.2). In these experiments, the number of condensers was increased to two to collect the liquid produced in two separate flasks as wax and oil. By reducing the operation parameters to two, three different $N_2$ flow rates and feeding rates were determined. The conversion of at least 86.8 wt.% was achieved in 9 experiments performed under selected conditions. Table 4.5 shows the product yields and conversions of thermal pyrolysis of the PO mixture.

Table 4. 5. Product yields and conversion of PO mixture pyrolysis.

| | Yield, wt.% | | | |
|---|---|---|---|---|
| **Run** | **Liquid** | **Gas** | **Solid-Residue** | **Conversion, wt.%** |
| **1** | 69.3 | 22.8 | 7.8 | 92.2 |
| **2** | 69.4 | 22.6 | 8.0 | 92.0 |
| **3** | 66.2 | 25.1 | 8.6 | 91.4 |
| **4** | 67.7 | 21.8 | 10.5 | 89.5 |
| **5** | 58.4 | 28.4 | 13.2 | 86.8 |
| **6** | 69.7 | 26.3 | 4.0 | 96.0 |
| **7** | 71.3 | 21.0 | 7.7 | 92.3 |
| **8** | 70.0 | 22.7 | 7.3 | 92.7 |
| **9** | 71.0 | 22.4 | 6.6 | 93.4 |
| **W** | 64.6 | 28.7 | 6.8 | 93.2 |

The effect of increasing the feeding rate on product distribution was investigated by keeping the $N_2$ flow rate constant at 900 mL/min in the Run 1-3 range. The first two experiments did not reveal very different results from each other, they obtained 92.2 wt.% and 92.0 wt.% conversion, and 69.3 wt.% and 69.4 wt.% liquid yields, respectively. As a result of the increase from 0.5 g/min feeding rate to 1 g/min, the amount of liquid and residue increased and the amount of gas decreased relatively. But later, with the use of 1.5 g/min feeding rate, the conversion decreased to 91.4 wt.% and the liquid yield decreased to 66.2 wt.%. In addition, the amount of noncondensable gas and residue were increased. As a result of these three experiments, it was clearly seen that the conversion decreased because of the increase in feeding rate. Namely, these were due to the increased feeding amount when using an equal period of time. Although a small increase was observed in the amount of liquid while passing from Run 1 to 2, the amount of gas was higher due to the fact that the vapours formed by the 7.5-gram plastics spent a lot of time in the reactor (also it may be caused by insufficient purging). In Run 3, on the other hand, it was seen that there was not enough time left for 22.5 grams of plastic to break apart at the same frequency of feeding.

Run 4-6 experiments, which were examined under the effect of 1000 mL/min $N_2$ flow rate, reached 89.5 wt.%, 86.8 wt.% and 96.0 wt.% conversions, respectively. Run 4 yielded 67.7 wt.% liquid, 21.8 wt.% gas and 10.5 wt.% residue. As a result of the Run 5 experiment, the amount of residue increased even more and the amount of liquid decreased up to 58.4 wt.%. In the Run 6 experiment, the remaining residue according to 0.5 g/min feeding rate was cracked, and liquid and gas amounts were increased to 69.7 wt.% and 26.3 wt.%, respectively. In these three experiments, a decreasing conversion

response was not observed as the feeding rate increased, as in the experiments in the first group. Based on this situation, experiments with common feeding rates but variable $N_2$ flow rates were compared. For example, when Run 1 and 4 were compared, the increased $N_2$ flow rate had a negative effect on conversion and therefore on fluid yield. Also, when Run 2 and 5 were compared, it was observed that the increasing $N_2$ flow rate decreased the conversion and liquid yield. However, unlike these, the increased $N_2$ flow rate while passing from Run 3 to Run 6, both increased the conversion and provided the highest liquid yield among the first 6 experiments.

Polyolefins were pyrolyzed under 1100 mL/min $N_2$ flow rate in the range of Runs 7-9. Contrary to what was seen in the first three experiments, conversions increased to 92.3 wt.%, 92.7 wt.%, and 93.4 wt.%, respectively, as the feeding rate increased. In addition, the highest liquid yield among all experiments was obtained with these experiments. Run 7 yielded 71.3 wt.% liquid and 21.0 wt.% gas, Run 8 produced 70.0 wt.% liquid, 22.7 wt.% gas, and Run 9 produced 71.0 wt.% liquid and 22.4 wt.% gas, respectively. Since the amounts of gas and liquid produced were very close to each other, the determinant between these three experiments was the amount of residue, namely conversion. In addition, when comparing Run 1, 4, and 7 experiments with 30 grams of feedstock, with the increasing $N_2$ flow rate from 900 mL/min to 1000 mL/min, liquid yield and conversion decreased, but when the $N_2$ flow rate increased to 1100 mL/min, liquid yield and conversion increased. In thermal pyrolysis experiments performed with 60 grams of feedstock (Run 2, 5, 8), again as the $N_2$ flow rate increased, conversion and liquid yield first decreased and then increased. However, in Run 3, 6, and 9 experiments where 90 grams of PO mixture was pyrolyzed, the liquid yield increased regularly, although the conversion was more at Run 6 and 9 than in the 3rd experiment, the increase was not regular.

Runs 6, 8, and 9 yielded 96.0 wt.%, 92.7 wt.%, and 93.4 wt.% conversions, respectively. Run 6 produced 69.7 wt.% liquid, 26.3 wt.% gas and 4.0 wt.% residue. 70.0 wt.% liquid, 22.4 wt.% gas and 6.6 wt.% residue were collected under Run 8 experimental conditions. With Run 9, it was observed that 71.0 wt.% liquid, 22.4 wt.% gas and 6.8 wt.% residue were produced. Although the highest liquid was produced by Run 7 (as 71.3 wt.%), Run 9 experiment was determined as the optimum condition for virgin PO mixture thermal pyrolysis (1100 mL/min $N_2$ flow rate, 1.5 g/min feeding rate) because Run 9 had a higher conversion.

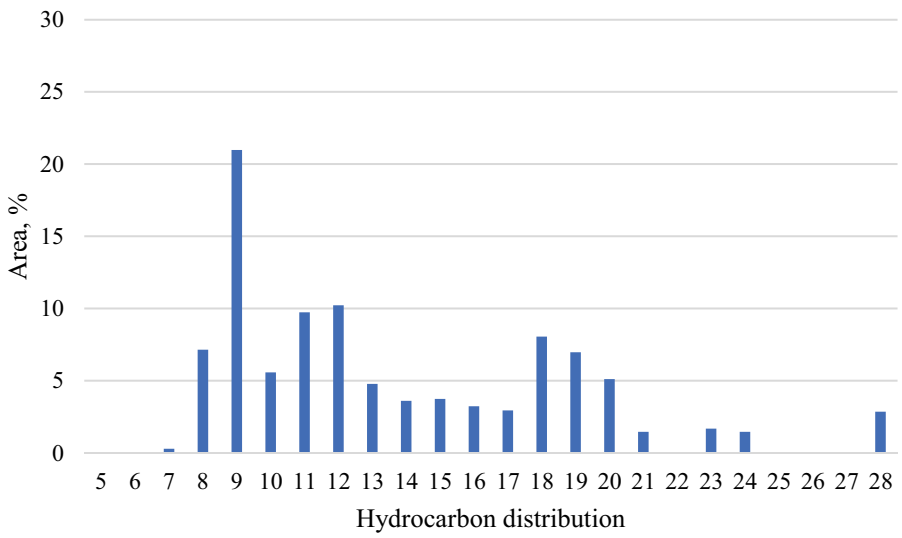


Figure 4. 7. Carbon number distribution of the liquid product of Run 9.

The hydrocarbon content of the liquid product was investigated by GC-MS analysis and it was understood that hydrocarbons were produced in the $C_7$-$C_{28}$ range (Figure 4.7). Thus, it was determined that the produced liquid consisted of 54.0% gasoline, 38.5% diesel and 7.5% wax according to the hydrocarbon distribution (Figure 4.8).

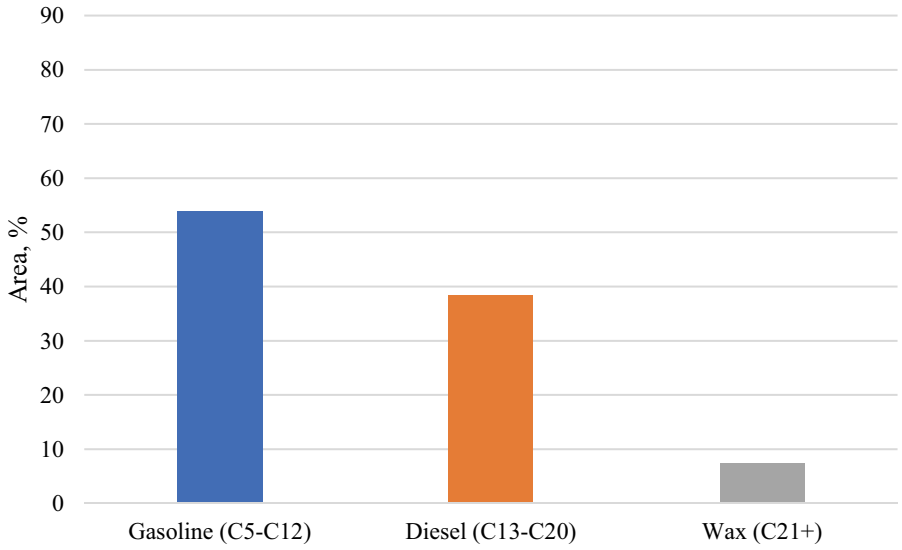


Figure 4. 8. Liquid product composition of Run 9 according to hydrocarbon range.

In addition, a test experiment was conducted to compare the liquid products produced by virgin and waste feedstock. Thermal pyrolysis of the waste polyolefin mixture was carried out under the determined optimum conditions (1100 mL/min $N_2$ flow

rate, 1.5 g/min feeding rate). From the thermal pyrolysis of the waste PO mixture, with a conversion of 93.2 wt.%, 64.6 wt.% liquid was obtained as waxy form, while 28.7 wt.% gas and 6.8 wt.% residue were observed.

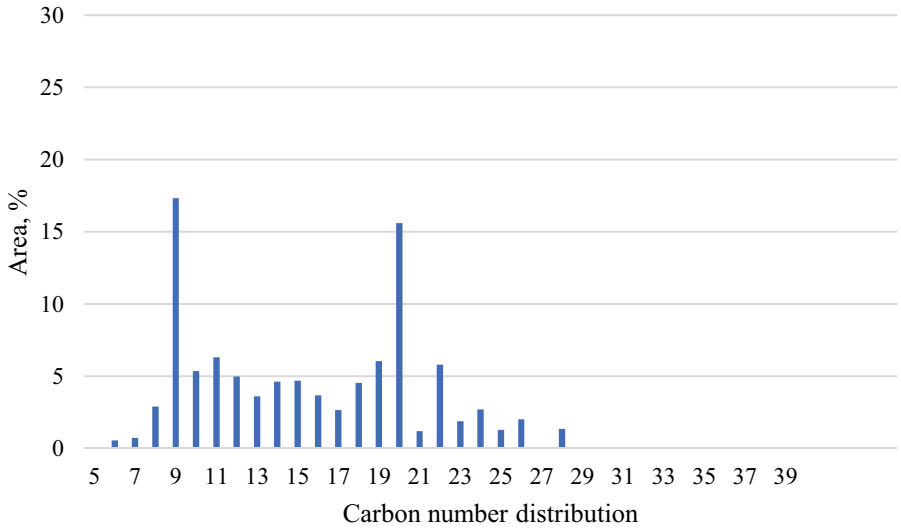


Figure 4. 9. Carbon number distribution of the liquid product of waste PO mixture.

As a result of GC-MS analysis of waste polyolefin pyrolysis liquid (Figure 4.9), it was seen that hydrocarbons were produced in the $C_5$-$C_{28}$ range. Thus, it was determined that the produced liquid consisted of 38.2% gasoline, 45.5% diesel and 16.3% wax according to the hydrocarbon distribution (Figure 4.10).

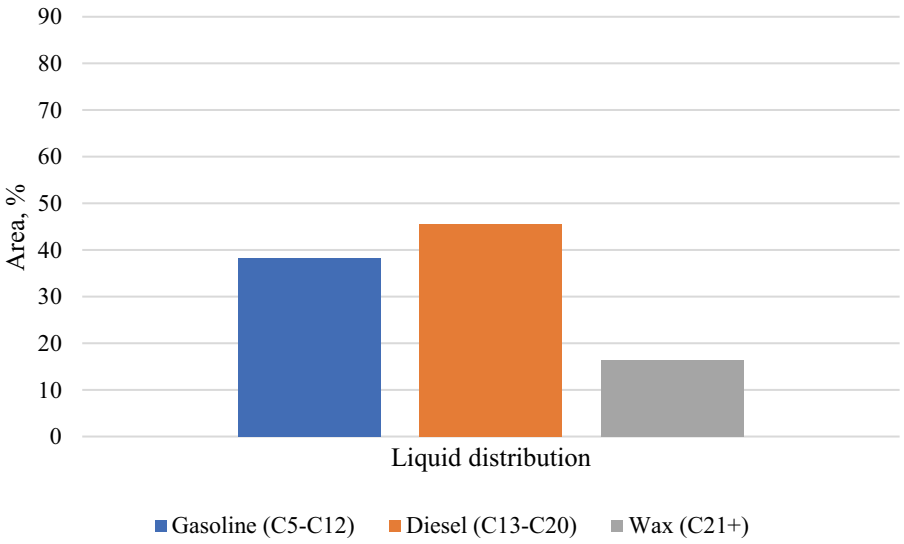


Figure 4. 10. Liquid product composition of waste PO mixture according to hydrocarbon range.

Although the hydrocarbon range of the liquid obtained from the waste PO mixture was narrower, it has been observed that the gasoline ratio produced by the virgin PO mixture liquid was higher. Run 9 mostly produced gasoline range hydrocarbons, while RunW mainly produced diesel range hydrocarbons. However, although the waste polyolefins conversion was high, the amount of liquid was less and it had a higher wax content than virgin PO mixture pyrolysis. Both products did not contain BTEX aromatics. Therefore, if these liquid products were to be used as raw materials in the refinery, the carbon number distribution and hydrocarbon content should be reduced. For this, a higher temperature thermal pyrolysis can be performed while keeping the other conditions the same.

### 4.2.2. Pyrolysis set-up operating batch-wise

The feedstocks prepared from 5 grams of virgin polyolefin mixture were thermally pyrolyzed by using three different $N_2$ flow rates (100 mL/min, 150 mL/min, 200 mL/min). It was observed that as the $N_2$ flow rate increased, the amount of liquid decreased, while the formation of wax in the liquid increased. In addition, the amount of residue remaining in the thermal reactor was increased, namely, conversion was decreased. While T2 and T3 obtained 50.97 wt.% and 45.61 wt.% liquid respectively, the highest liquid efficiency of approximately 57 wt.% was produced by T1. For this reason, the T1 (100 mL/min) experiment was determined as the optimum condition. Product yields and conversion of the PO mixture are specified in Table 4.6.

Table 4.6. Product yields and conversion of PO mixture pyrolysis in a batch-operated set-up.

| | **Yield, wt.%** | | | | |
|---|---|---|---|---|---|
| | **Liquid** | | **Noncondensable Gas** | **Residue** | **Conversion, wt.%** |
| **Run** | **Wax** | **Oil** | | | |
| **T1** | 11.28 | 45.69 | 42.00 | 1.03 | 98.97 |
| **T2** | 13.57 | 37.40 | 47.49 | 1.56 | 98.45 |
| **T3** | 15.04 | 30.57 | 52.70 | 1.69 | 98.31 |

Carbon number distributions of the liquid produced from thermal experiments were investigated by GC-MS analysis. Figure 4.11 shows the hydrocarbon distribution depending on the peak areas.

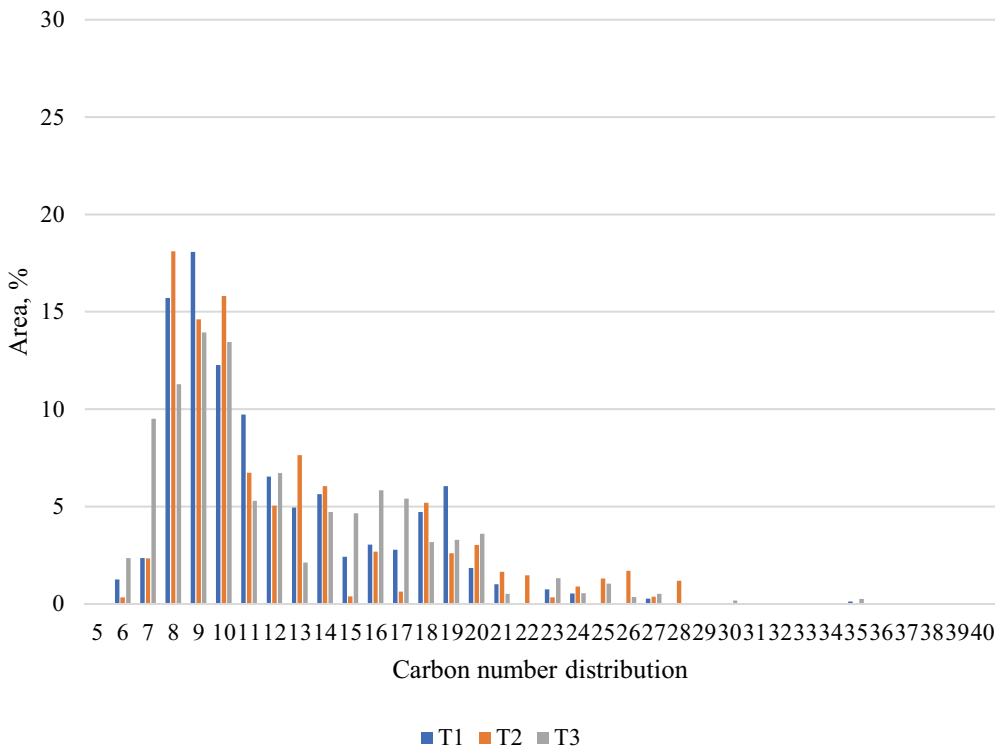


Figure 4. 11. Carbon number distribution of the liquid product obtained by thermal pyrolysis of PO mixture.

When the three thermal pyrolysis liquids of the polyolefin mixture were examined, it was observed that the number of gasoline-like products decreased slightly as the $N_2$ flow rate increased (Figure 4.12). Diesel-like products, on the other hand, decreased while passing from T1 to T2, and reached their maximum value at T3.

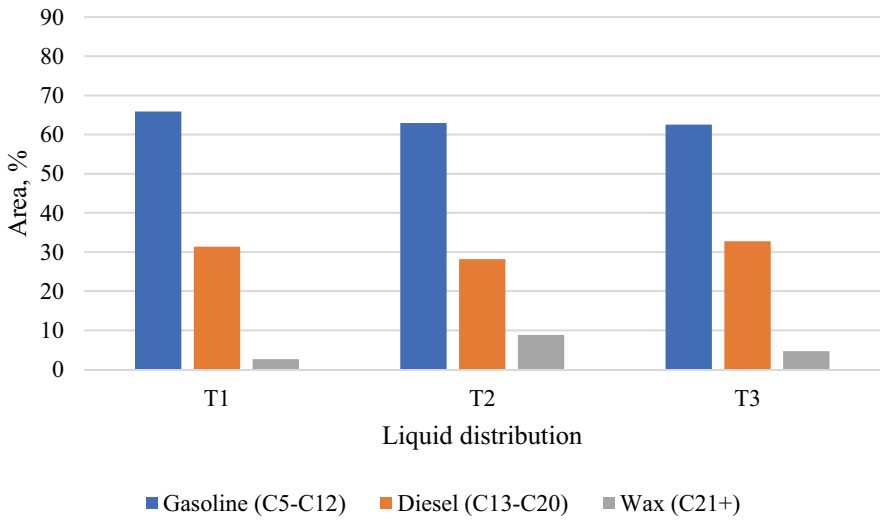


Figure 4. 12. Distribution of thermal pyrolysis liquids according to the hydrocarbon range.

## 4.3. Catalytic Pyrolysis

Prior to each experiment, ammonium-based zeolites were calcined at 550 ℃ for 5 hours to obtain hydrogen form, increase the acidity of the catalyst, and supply an efficient cracking of polyolefins.

### 4.3.1. In-situ Catalytic Pyrolysis (CP) of LDPE (for the ISMO-22 Conference)

In-situ catalytic pyrolysis of virgin LDPE polyolefin was scrutinized for the ISMO-22 conference (Fatma Defne Çalık 2022). For this study, ZSM-5 (30) and Silica-alumina (30) catalysts were tested in different catalyst-to-plastic ratios. Primarily, liquids produced by Run 5 of the LDPE thermal pyrolysis (Section 4.2.1.) were chosen as a basis. The aim was cracking waxy hydrocarbons into lighter ones (i.e. gasoline, diesel range) via in-situ catalytic pyrolysis.

The effect of the ZSM-5 (30) catalyst was investigated at 1/100, 1/500 and 1/1000 catalyst/plastic ratios, respectively. It was observed that the amount of liquid increased as the amount of catalyst decreased. However, while the amount of liquid increased, wax formation began to be observed in the liquid after a 1/100 catalyst-to-plastic ratio. Therefore, the 1/250 catalyst-to-plastic ratio was taken into account and produced 38.7 wt.% liquid, 61.2 wt.% gas and 0.2 wt.% coke-residue. Although the obtained liquid was less than those produced at 1/500 and 1/1000 ratios, this condition was considered optimum since the aim was to obtain the maximum liquid by eliminating wax production. Afterwards, the Silica-alumina (30) catalyst produced within the scope of this thesis was performed with a 1/250 catalyst/plastic ratio. As a result, 69.6 wt.% pyrolysis liquid (oil), 15.8 wt.% gas and 14.6 wt.% coke residue were collected. All the product yields and conversions can be seen in Table 4.7.

Table 4.7. Product distribution and conversion of non-catalytic and in-situ catalytic LDPE pyrolysis.

| | | | Yield, wt.% | | | |
|---|---|---|---|---|---|---|
| **Run** | **Catalyst** | **Catalyst/plastic ratio** | **Liquid** | **Gas** | **Coke, Residue** | **Conversion, wt.%** |
| **5** | Thermal | 0 | 77.7 | 20.6 | 1.7 | 98.3 |
| **5.1** | ZSM-5 (30) | 1/100 | 32.0 | 67.8 | 0.2 | 99.8 |
| **5.2** | ZSM-5 (30) | 1/500 | 42.7 | 56.9 | 0.4 | 99.6 |
| **5.3** | ZSM-5 (30) | 1/1000 | 45.3 | 54.2 | 0.5 | 99.5 |
| **5.4** | ZSM-5 (30) | 1/250 | 38.7 | 61.2 | 0.2 | 99.8 |
| **5.5** | Silica-alumina (30) | 1/250 | 69.6 | 15.8 | 14.6 | 85.4 |

The liquid produced with Run 5.4 and 5.5 were analyzed by GC-MS. Run 5.4 produced hydrocarbons in the $C_6$-$C_{24}$ range, while Run 5.5 produced hydrocarbons in the $C_7$-$C_{27}$ range. When the hydrocarbon distribution graph of Run 5.4 was examined, it was clearly seen that the vast majority consists of lighter ($C_6$-$C_{12}$) hydrocarbons (Figure 4.13).

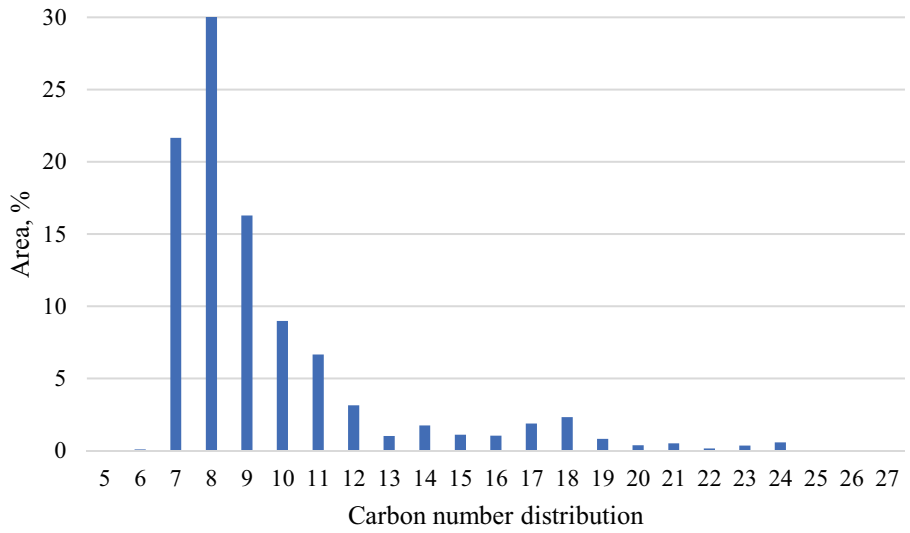


Figure 4. 13. Carbon number distribution of the liquid produced via ZSM-5 (30) catalyst.

When the hydrocarbon distribution of Run 5.5 was investigated, it was observed that the $C_{13}$-$C_{21}$ range was more intense, but almost the same amount as the lighter carbon numbers (Figure 4.14).

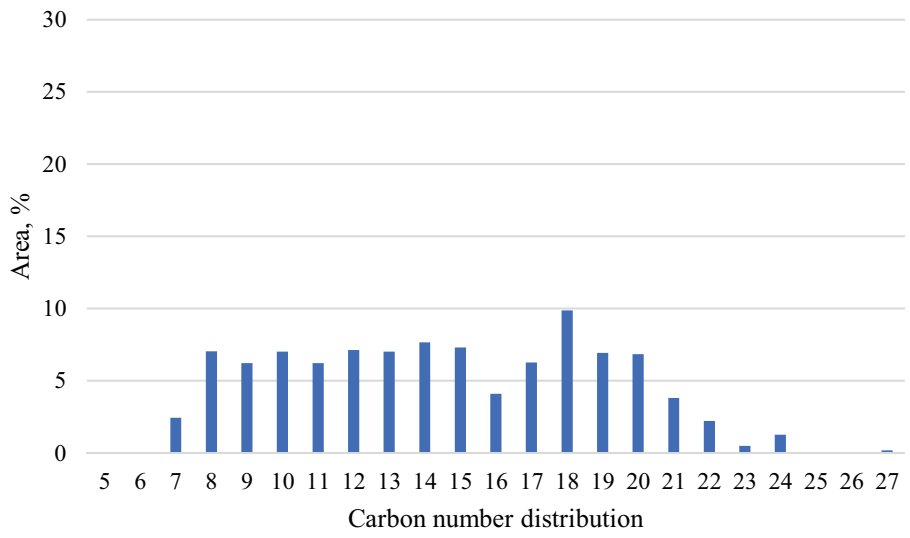


Figure 4. 14. Carbon number distribution of the liquid produced via silica-alumina (30) catalyst.

The distribution of liquids obtained from thermal pyrolysis and in-situ catalytic pyrolysis experiments in the presence of ZSM-5 (30) and Silica-alumina (30) catalysts, according to hydrocarbon ranges, is shown in the graph (Figure 4.15). It was observed that both catalysts increased the amount of gasoline (88.24%, and 36.1%, respectively), and decreased the amount of diesel (10.22%, 55.97%, respectively) and wax (1.54%, and 7.93% respectively). Also, it was observed that 9.9% benzene derivatives, 1.7% ethylbenzene, 3.1% toluene and 8.2% p-xylene aromatics were produced by the reactions of ZSM-5 (30) catalyst. In addition, 0.1% benzene derivative was produced with a silica-alumina (30) catalyst.

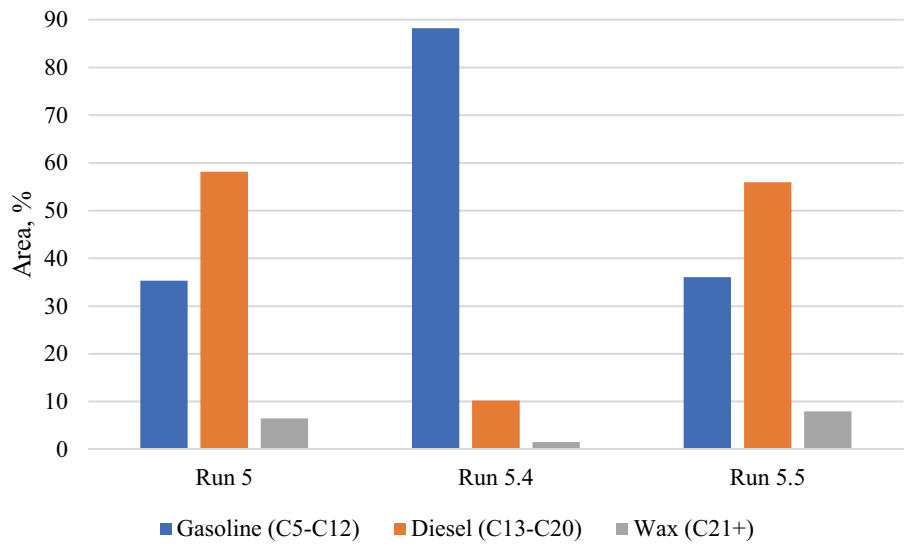


Figure 4. 15. Distribution of the runs 5, 5.4 and 5.5 for non-catalytic and in-situ catalytic pyrolysis of LDPE according to the hydrocarbon range.

In this study, it was found that the ZSM-5 and silica-alumina catalysts were compatible with the in-situ catalytic pyrolysis method and they could convert the waxy product into nonviscous oil. At the same time, the contents of the liquid produced were also improved through catalytic reactions. The excess amount of aromatics in the liquid produced by the ZSM-5 catalyst in the Run 5.4 experiment may need to be reduced so that it can be used as a raw material in the refinery later on. At the same time, it was promising that the silica-alumina catalyst produced a liquid product more than Run 5.4 and closer to that produced in thermal pyrolysis. Adversely, the conversion of Run 5.5, 85.4 wt.%, was lower than in all experiments due to the amount of residue-coke. To reduce this, experiments can be performed by increasing the amount of silica-alumina or pyrolysis temperature, or the product distribution can be observed by extending the duration.

### 4.3.2. Ex-situ Catalytic Pyrolysis (CP) of PO Mixture

Ex-situ catalytic pyrolysis of virgin polyolefin mixture was carried out with three different catalysts (ZSM-5 (50), silica-alumina (50), silica-alumina (50) via ZSM-5 (50)) and two different WHSV (500 $h^{-1}$, 200 $h^{-1}$). By the thermal experiment T1 (100 mL/min), 57 wt.% liquid, 42 wt.% noncondensable gas and 1 wt.% residue were obtained. While 45.7 wt.% of the produced liquid was oil, 11.3 wt.% was wax. It was investigated how catalyst types and catalyst-to-plastic ratios affected the quantity and the quality of the

product. Coke formation was observed on the catalysts in the catalytic experiments. The distribution of products and conversion are indicated as weight % in Table 4.8.

Table 4.8. Product distribution and conversions of ex-situ catalytic pyrolysis experiments.

| | | | Yield (wt.%) | | | | | |
|---|---|---|---|---|---|---|---|---|
| | | | Liquid | | Gas | Residue | Solid | Conversion, wt.% |
| **Run** | **Catalyst type** | **WHSV ($h^{-1}$)** | **Wax** | **Oil** | | | | |
| **T1** | Thermal (Non-catalytic) | 0 | 11.3 | 45.7 | 42.0 | 1.0 | 0.0 | 99.0 |
| **ES1** | ZSM-5 (50) | 500 | 8.6 | 27.3 | 62.6 | 1.0 | 0.5 | 98.5 |
| **ES2** | ZSM-5 (50) | 200 | 7.9 | 22.0 | 68.1 | 1.3 | 0.8 | 97.9 |
| **ES3** | Silica-alumina (50) | 500 | 9.6 | 47.0 | 41.5 | 1.1 | 0.8 | 98.1 |
| **ES4** | Silica-alumina (50) | 200 | 9.3 | 44.8 | 43.7 | 1.3 | 0.8 | 97.9 |
| **ES5** | Silica-alumina (50) via ZSM-5 (50) | 500 | 7.0 | 38.2 | 52.2 | 1.0 | 1.6 | 97.4 |
| **ES6** | Silica-alumina (50) via ZSM-5 (50) | 200 | 10.2 | 47.7 | 40.8 | 0.7 | 0.6 | 98.7 |

In the experiment ES1 where ZSM-5 (50) catalyst was applied with 500 $h^{-1}$ WHSV, the amount of liquid decreased to 36 wt.%, and it included 8.6 wt.% wax and 27.3 wt.% oil. The amount of noncondensable gas increased to 65.6 wt.%, and the residue was 1 wt.%. In addition, 0.5 wt.% coke formation was observed. The graph showing the hydrocarbon distribution of the produced thermal and catalytic pyrolysis fluids is given in Figure 4.16. As can be seen in this graph obtained by GC-MS, in the ES1 experiment, the pyrolysis vapour was cracked more than in the thermal experiment. Hydrocarbons were mostly produced in the $C_5$-$C_{12}$ range (gasoline) which was 65.9% from thermal pyrolysis, and 80.3% from catalytic pyrolysis. In addition, while valuable aromatics such as benzene, toluene, and xylene were not produced in the thermal experiment, the liquid produced with ES1 included approximately 5 wt.% aromatics (2.6% benzene derivatives and 2.3% o-xylene).

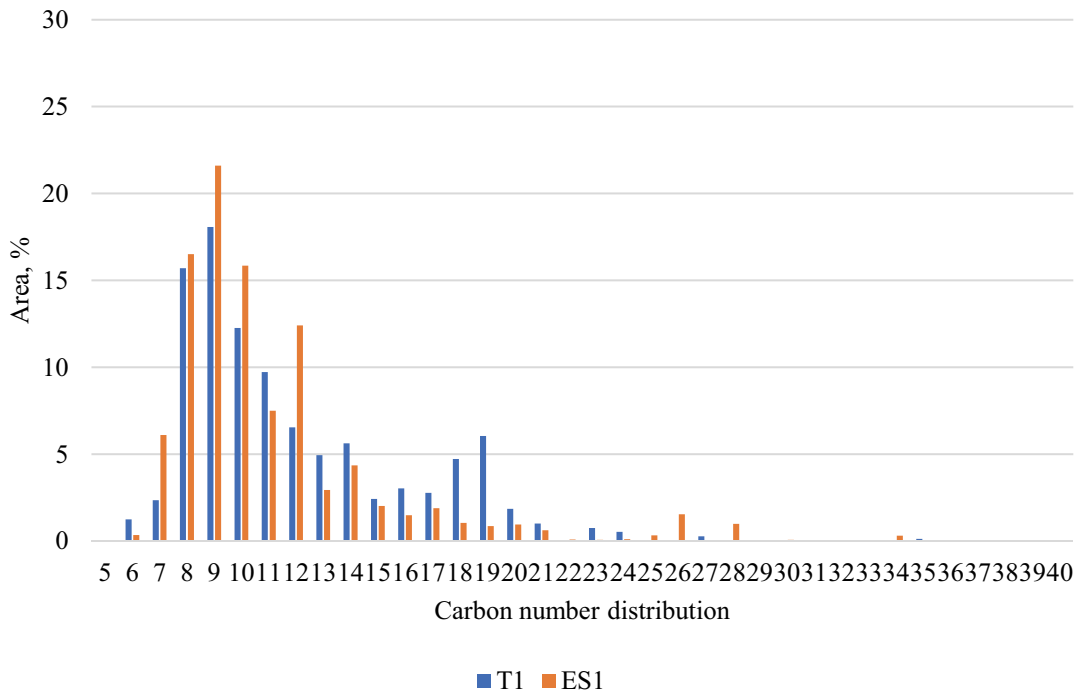


Figure 4. 16. Carbon number distribution of T1 and ES1.

In the ES2 experiment, ZSM-5 (50) catalyst was used with 200 $h^{-1}$ WHSV. In this experiment, the liquid decreased to 30 wt.% and the noncondensable gas increased to 68.1 wt.%. While 7.9 wt.% wax was produced, the amount of oil was 22 wt.%. The residue and coke formation increased to 1.3 wt.% and 0.8 wt.%, respectively. The rise in the amount of catalyst provided more cracking and increased the amount of gasoline to 82.8%. In the liquid produced with ES1, hydrocarbons were contain up to 34 carbon compounds, while ES2 produced compounds with a maximum of 25 carbons (Figure 4.17). Besides, the obtained pyrolysis liquid contains 0.8% ethylbenzene, 4.3% benzene derivatives and 3.7% p-xylene.

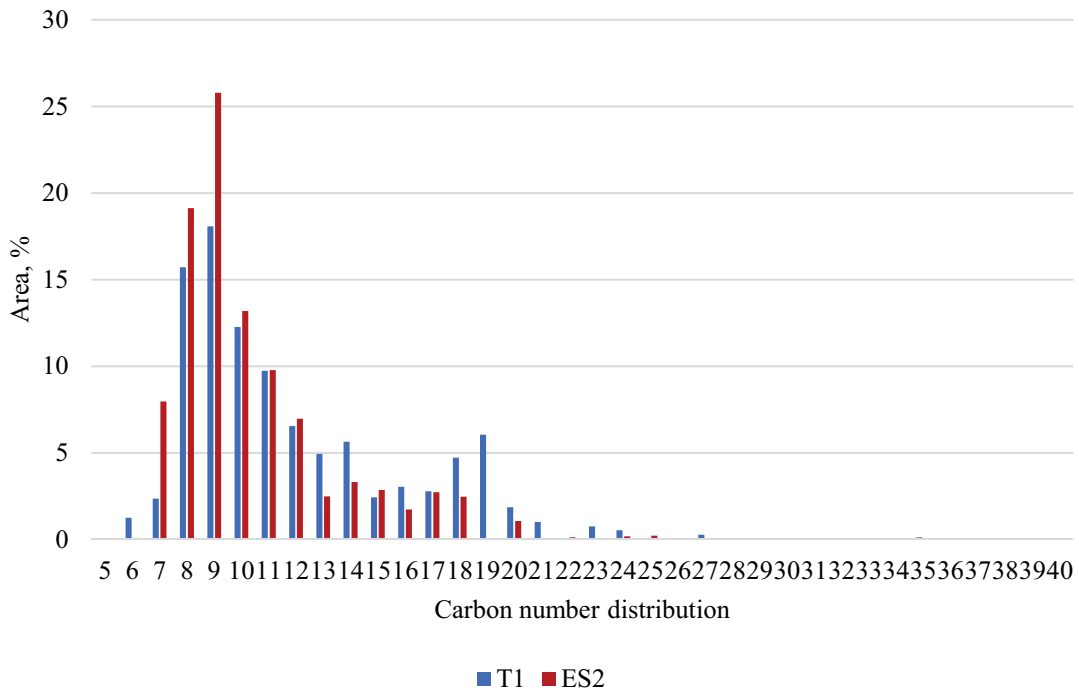


Figure 4. 17. Carbon number distribution of T1 and ES2.

56.6 wt.% liquid (9.6 wt.% wax, 47.0 wt.% oil) and 41.5 wt.% noncondensable gas were produced in the ES3 experiment in which silica-alumina (50) catalyst produced based on commercial zeolite, with 500 $h^{-1}$ WHSV. In this catalytic experiment, the amount of wax decreased, and oil increased compared to thermal pyrolysis. The amount of residue and coke obtained was 1.1 wt.% and 0.8 wt.%, respectively. Except for the change in the liquid product, the T1 and ES3 experiments were very similar. In addition, the amount of diesel remained almost the same, while the amount of gasoline increased to 66.23% (Figure 4.18).

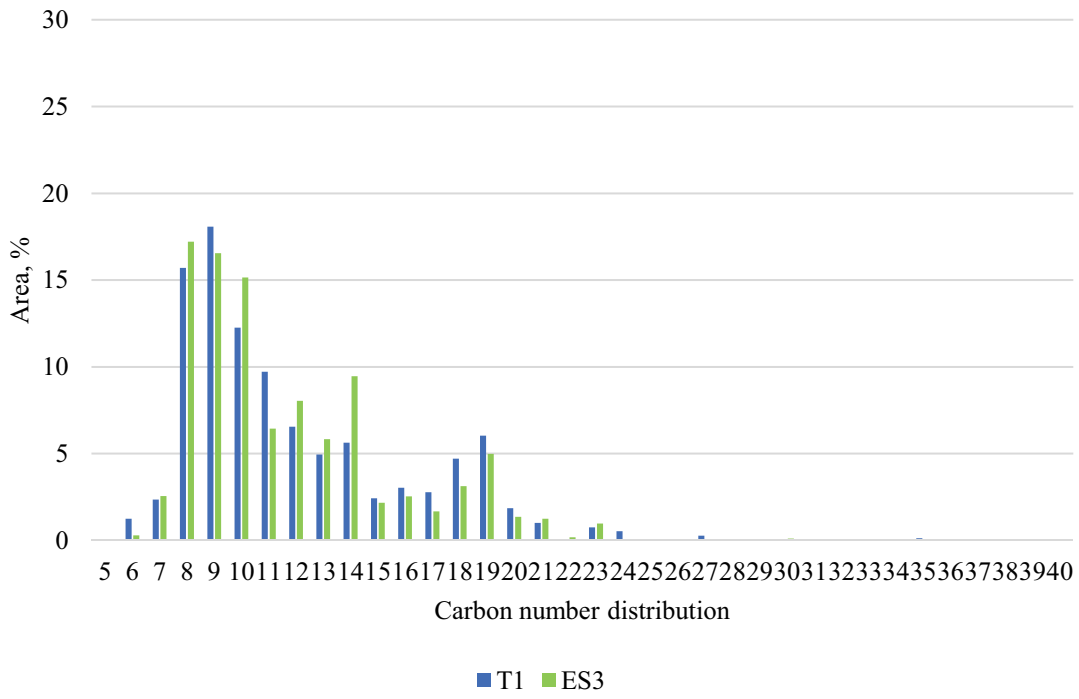


Figure 4. 18. Carbon number distribution of T1 and ES3.

In the ES4 experiment, 200 $h^{-1}$ WHSV was tested again using a silica-alumina (50) catalyst. Compared to T1, the amount of liquid decreased to 54.2 wt.% (9.3 wt.% wax, 44.8 wt.% oil), while the amount of gas increased to 43.7 wt.%. While 1.3 wt.% residue was obtained, coke formation was determined as 0.8 wt.%. As a result of this experiment, it was observed that both gasoline and diesel range hydrocarbons decreased, and waxes increased to 5.93% (Figure 4.19). When the catalyst was increased in the E4 compared to the ES3, more cracking was expected, but the opposite situation was detected. Also, the conversion was the same as the ES2 experiment, and lower than T1.

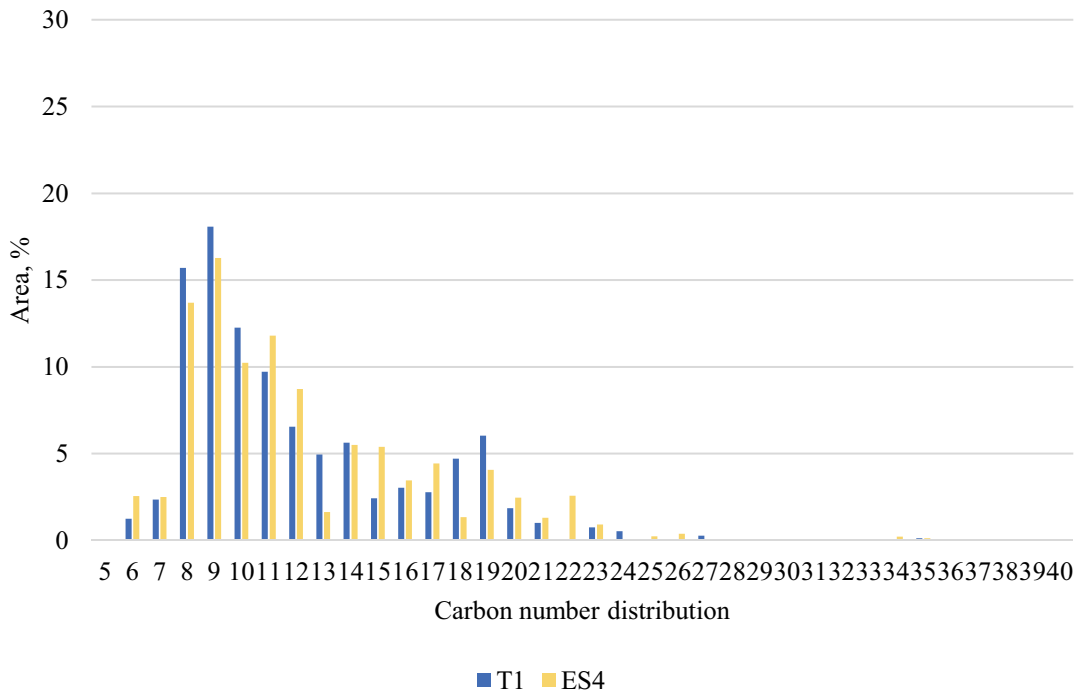


Figure 4. 19. Carbon number distribution of T1 and ES4.

In this new ex-situ catalytic experiment, E5, the behaviour of a new catalyst (Silica-alumina (50) via ZSM-5 (50)), produced from zeolite and silica-alumina catalysts used in previous experiments, was investigated. Thanks to this catalyst working at 500 $h^{-1}$ WHSV, the amount of liquid was determined as 45.2 wt.% (7.0 wt.% wax, 38.2 wt.% oil) and the amount of noncondensable gas as 52.2 wt.%. While the residual was 1 wt.%, coke formation reached its highest value in all experiments at 1.6 wt.%. When the content of the liquid products was examined, it was observed that the gasoline and diesel range slightly decreased compared to T1, while the amount of wax composition increased to 4.26% (Figure 4.20). In other words, it was very similar to the ES4 experiment in terms of composition.

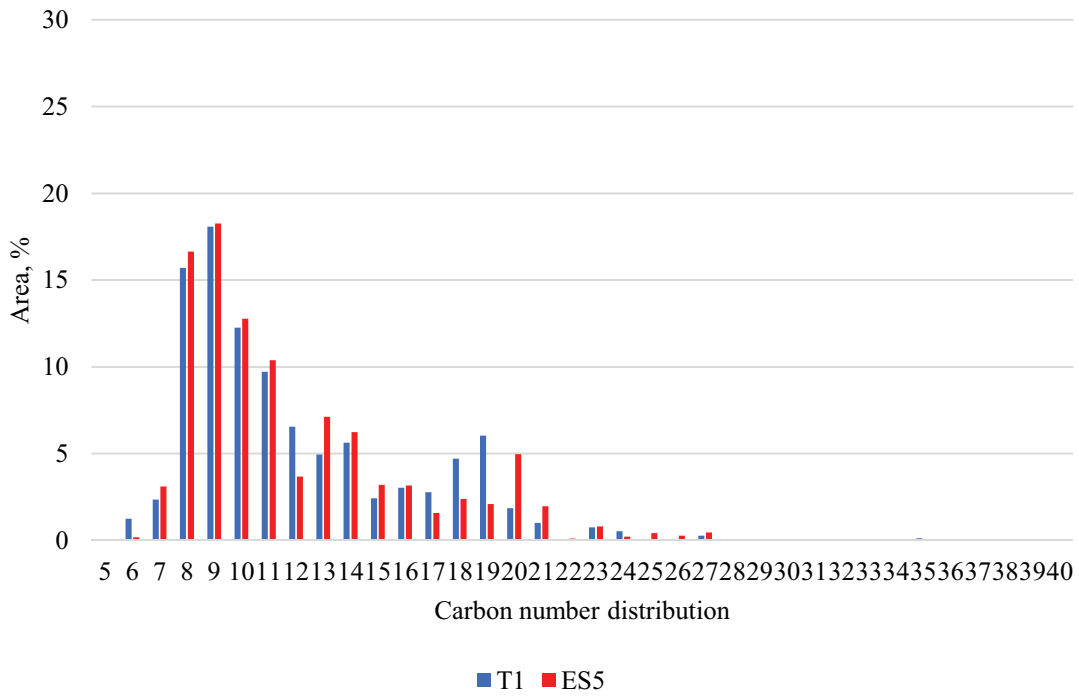


Figure 4. 20. Carbon number distribution of T1 and ES5.

In the sixth ex-situ catalytic experiment, this experimental set was completed by using 200 $h^{-1}$ WHSV. While a decrease in the amount of liquid was expected compared to the thermal test and the ES5, the liquid product increased to approximately 58 wt.%, unlike all the catalytic experiments. Gas, residue and coke amounts were calculated as 40.8 wt.%, 0.7 wt.% and 0.6 wt.%, respectively. When the obtained pyrolysis liquid was examined, as in the ES4 and ES5 experiments, gasoline and diesel range hydrocarbons decreased, while wax formation increased to 5.54% (Figure 4.21).

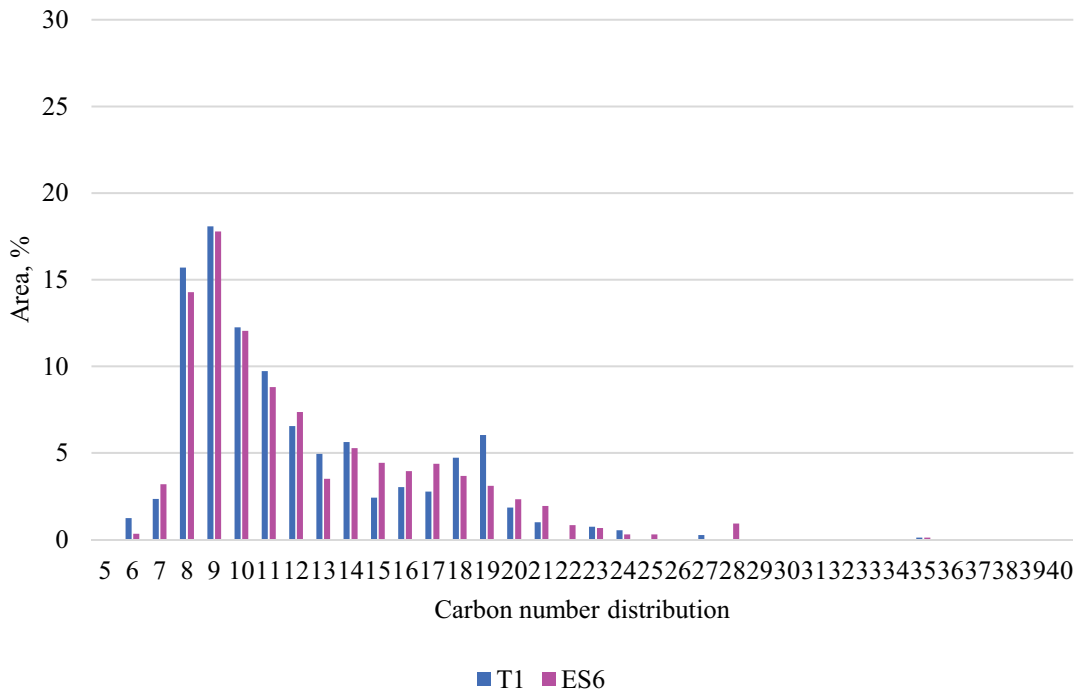


Figure 4. 21. Carbon number distribution of T1 and ES6.

All this product distribution and content were gathered under two separate graphs according to the effect of WHSV. As seen in Figure 4.22 the behaviours of ES1, ES3 and ES5 experiments at 500 $h^{-1}$ WHSV, respectively, were compared. While 65.9% of gasoline was produced by thermal experiment, ZSM-5 (50) (80.3%) and Silica-alumina (50) (66.23%) catalysts increased the amount of gasoline. In the ES5 experiment, the ZSM-5 (50) supported silica-alumina (50) catalyst reduced the gasoline content to 65%. Diesel range hydrocarbons decreased from 31.4% to 15.5%, 31.2% and 30.7%, respectively, in the three catalytic tests. While wax formation could be reduced from 2.7% to 2.6% with the Silica-alumina (50) catalyst, an increase in the effect of the other two catalysts was observed. Also, valuable BTEX aromatics could only be performed in the presence of ZSM-5 (50).

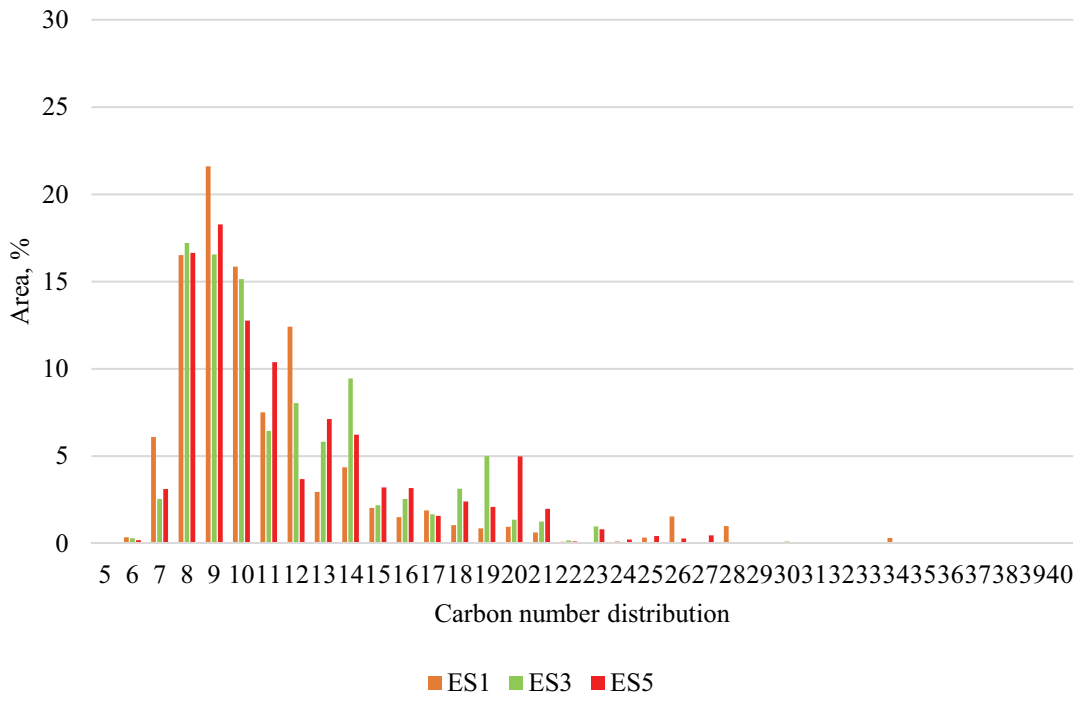


Figure 4. 22. Comparison of carbon number distributions of liquid produced by 500 $h^{-1}$ WHSV.

Another condition examined was 200 $h^{-1}$ WHSV, which was obtained by increasing the mass of the catalysts used. The results to be compared here were those of the ES2, ES4 and ES6 experiments (Figure 4.23). As in the 500 $h^{-1}$ condition, the amount of gasoline increased (82.8%) with the ZSM-5 (50) test, but in the presence of Silica-alumina (50) and Silica-alumina (50) via ZSM-5 (50) catalysts, it was decreased to 65.8% and 63.8%, respectively. As in the other experiments with 500 $h^{-1}$, the amount of diesel decreased to 16.6%, 28.3% and 30.7%, respectively, in the presence of all these three catalysts. While the wax composition decreased significantly to 0.5% in the presence of ZSM-5 (50), an increase of more than twice was observed in the other two catalytic experiments, on the contrary.

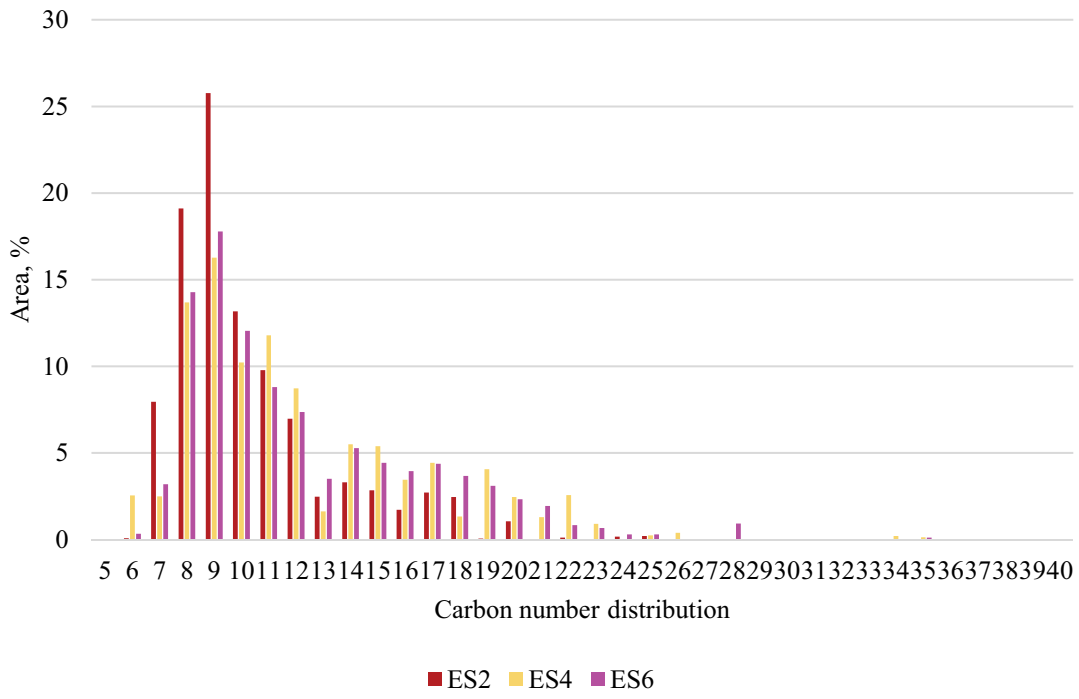


Figure 4. 23. Comparison of carbon number distributions of liquid produced by 200 $h^{-1}$ WHSV.

In Figure 4.24, the gasoline, diesel, and wax distributions of all liquids obtained from thermal and catalytic experiments are clearly indicated.

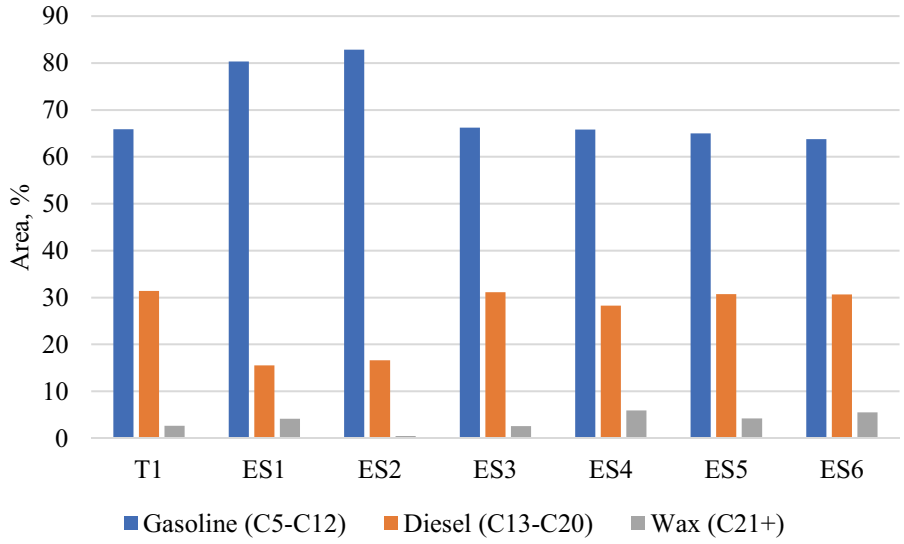


Figure 4. 24. Distribution of the thermal and ex-situ catalytic pyrolysis liquids according to the hydrocarbon range.

Increasing the production of intermediate products such as naphtha ($C_5$-$C_{12}$ paraffins) instead of fuel production from the pyrolysis of polyolefins, using them as raw

materials in the petrochemical industry to produce plastic monomers and providing economic feasibility should be supported. It is promising that the liquids obtained in this thesis experiment are also suitable for this context. However, the metals and additives in the waste polyolefins both reduce the quality of the product and are not suitable for feeding into the hydrocracking unit in the industry, and pretreatment is required. Studies on rapid deactivation and reuse problems of catalysts should be performed. In other words, existing catalysts for catalyst regeneration should be improved with factors such as support and promoter, and new types of catalysts should also be investigated (i.e. naphtha selective). In the light of all these experiments and literature review, the design of new reactors suitable for the equal heating and melting problem of plastics and the mass transfer limitation should be investigated (Nan Zhou 2021, Junya Nishino 2008).

## 4.4. Catalyst Characterization

According to $NH_3$-TPD results, ZSM-5 (30) and ZSM-5 (50) have total acidities as 539.11 μmol$NH_3$/g and 528.12 μmol$NH_3$/g, respectively. Silica-alumina (30) and silica-alumina (50) catalysts produced based on these two zeolite catalysts, have acidities of , and 484.66 μmol$NH_3$/g. In addition, ZSM-5 (50) supported silica-alumina (50) catalyst has an acidity of 496.91 μmol$NH_3$/g. When the peaks formed by desorption temperatures were examined, silica-alumina (50) and ZSM-5 supported silica-alumina (50) catalysts can be interpreted as weak acid, silica-alumina (30), ZSM-5 (30) and ZSM-5 (50) catalysts can be interpreted as strong acids. As Si/Al ratio increased (30 to 50), total acidity decreased among zeolites and silica-aluminas. At the same time, the strength of acid sites decreased. ZSM-5 zeolite, supported on silica-alumina catalyst, made the catalyst more acidic than silica-alumina (50). In addition, its acidic strength decreased. The total acidities of the catalysts are in the order silica-alumina (30), ZSM-5 (30), ZSM-5 (50), ZSM-5 (50) supported silica-alumina (50), and silica-alumina (50) from highest to lowest.

As a result of in-situ catalytic pyrolysis experiments conducted for the ISMO 2022 conference, silica-alumina (30) favored diesel-range hydrocarbons in the $C_{13}$-$C_{21}$ range, while ZSM-5 (30) was more selective in producing $C_6$-$C_{12}$ gasoline-range hydrocarbons. This behavior of the silica-alumina catalyst may be due to its strongly acidic nature. Because the catalyst was active at high temperatures (479 °C).

When ex-situ catalytic pyrolysis experiments were examined, ZSM-5 (50), ZSM-5 (50) supported silica-alumina (50), and silica-alumina (50) catalysts are more selective towards gasoline-range hydrocarbon production in common. However, the performances of ZSM-5 (50) supported silica-alumina (50), and silica-alumina (50) catalysts are very close to each other, and gasoline production was less and diesel production was higher than zeolites.

Spent catalysts were characterized by FTIR in transmission mode. It was clearly seen that there were coke depositions observed on all three catalysts. Figure 4.25 illustrates the chemical groups deposited on catalysts (Liangliang Fan 2021). No coke formation was detected on spent silica-alumina (50) catalysts collected after ES3 and ES4 experiments and on ZSM-5 (50) supported silica-alumina (50) obtained after ES6 experiment.

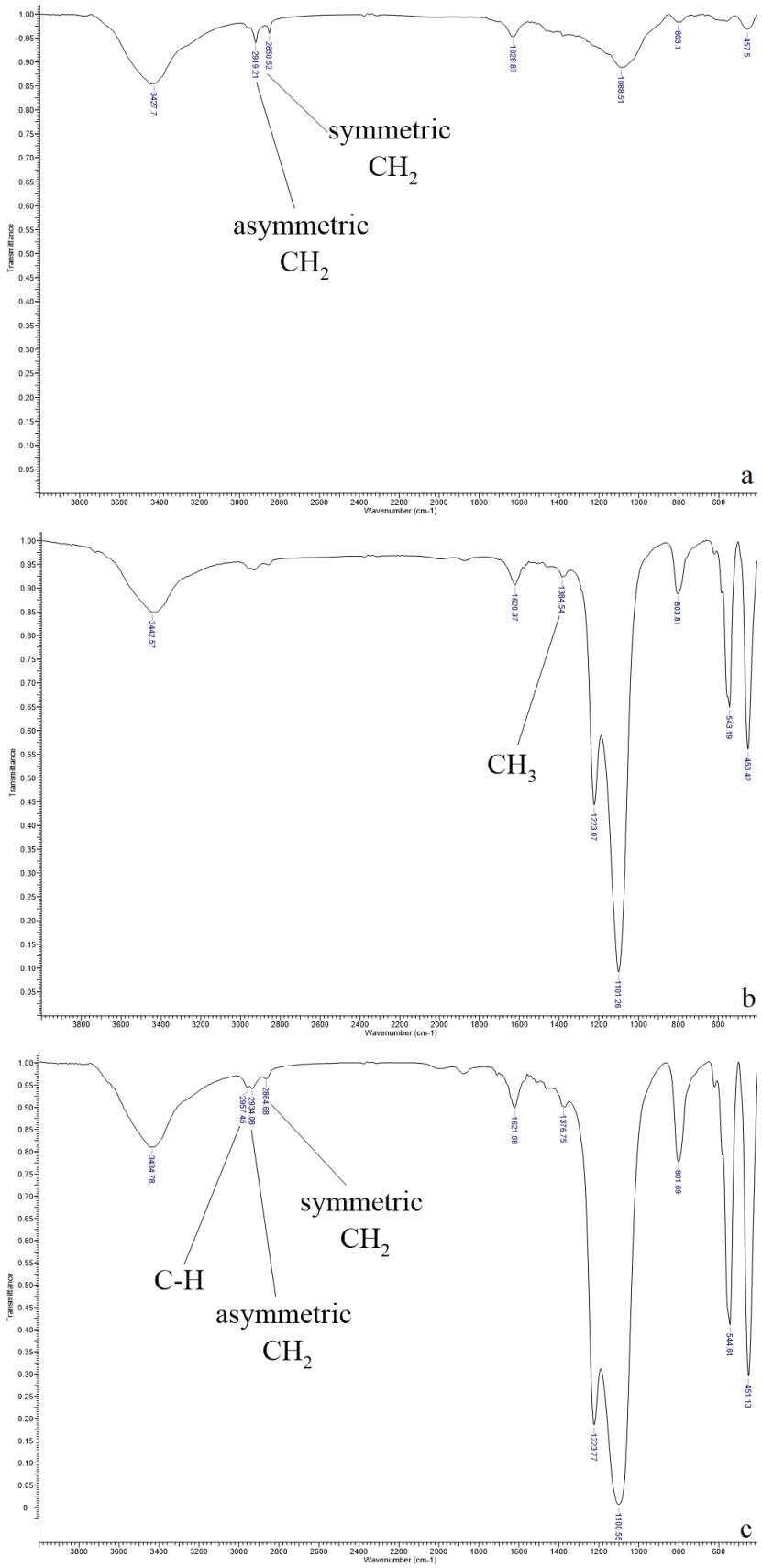


Figure 4. 25. FTIR results of spent a) ZSM-5 (Si/Al=50) supported silica-alumina ES5, b) ZSM-5 (Si/Al=50) catalysts ES1, c) ZSM-5 (Si/Al=50) catalysts ES2.

## 4.5. Product Characterization

The chemical structure of all liquids produced by thermal (Figure 4.26), and catalytic (Figure 4.27) experiments performed in the ex-situ CP unit was determined by FTIR-ATR. Thermal pyrolysis liquids showed consistent peaks among each other. Catalytic pyrolysis liquids also gave very close peaks to each other. Double bonds determined the presence of alkenes, and C-H bonds determined compounds according to the size of the peaks and the transmittance values to compare with GC-MS results.

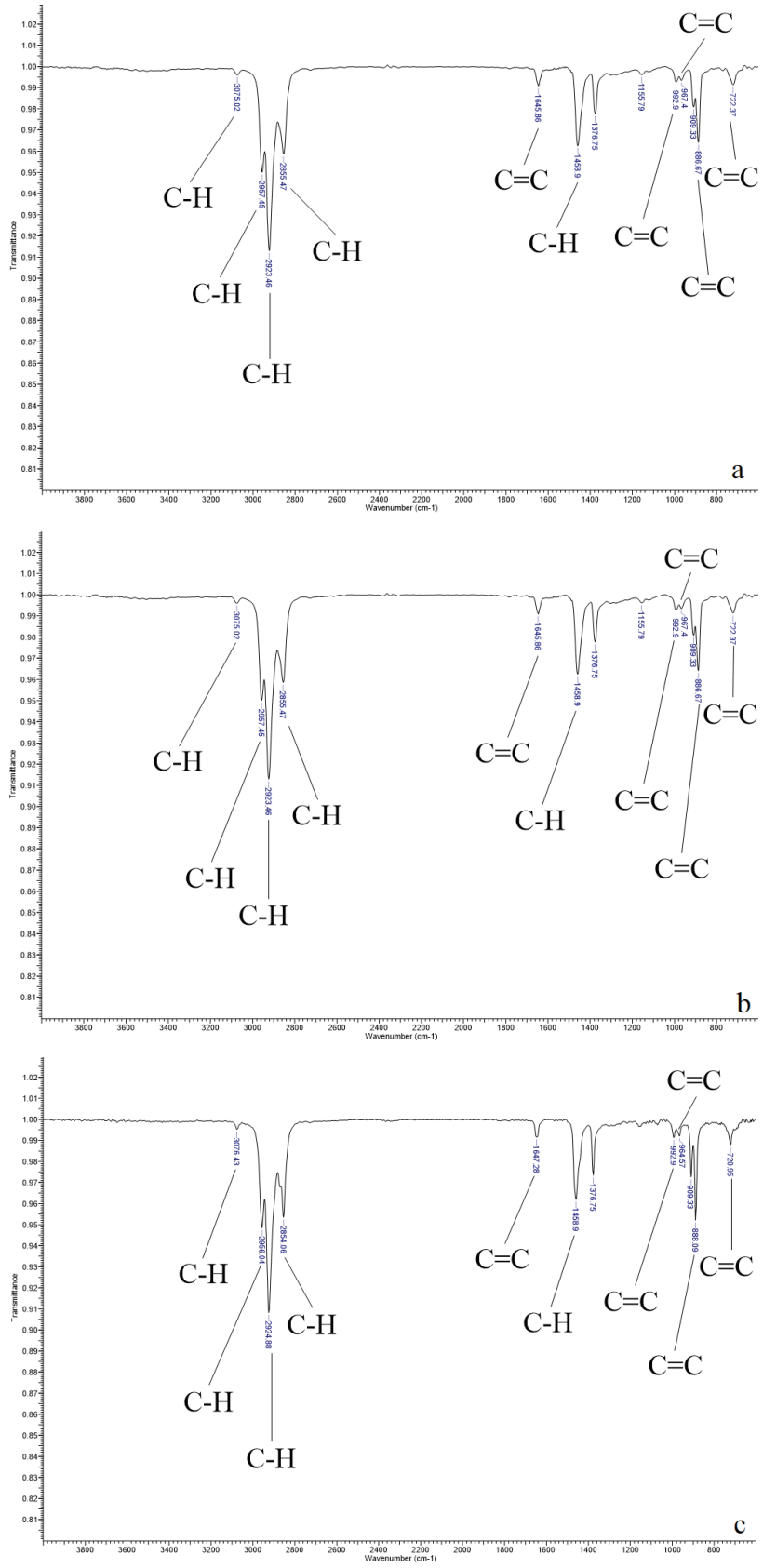


Figure 4. 26. FTIR results of non-catalytic pyrolysis oils a) T1, b) T2, c) T3.

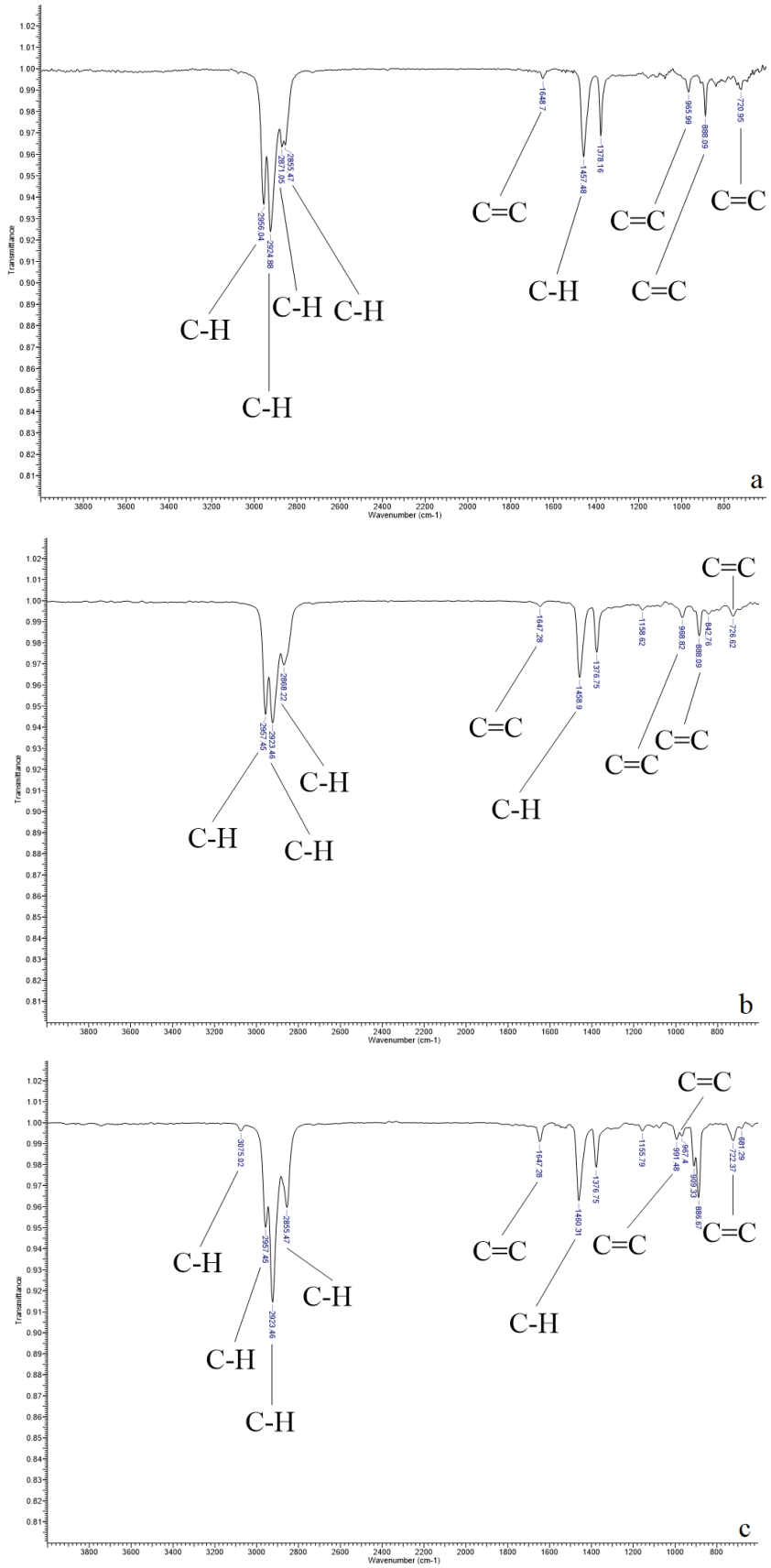


Figure 4. 27. FTIR results of ex-situ catalytic pyrolysis oils a) ES1, b) ES2, c) ES3, d) ES4, e) ES5, f) ES6.

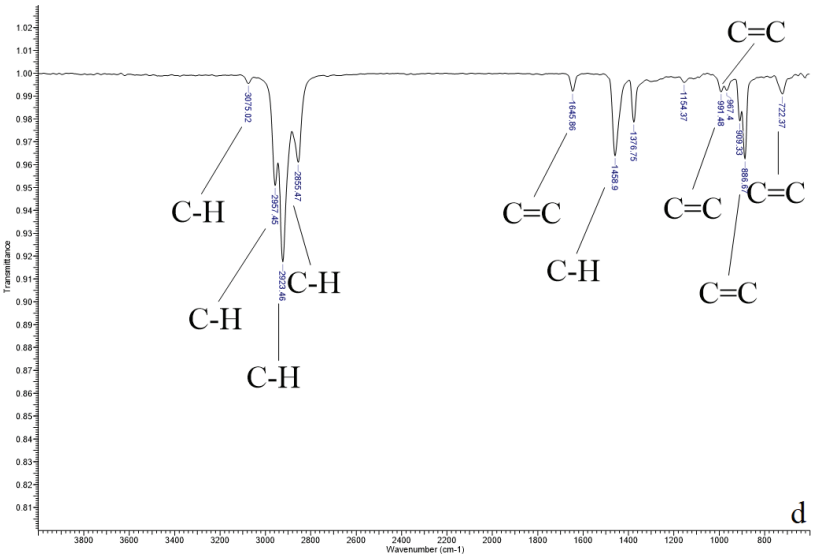


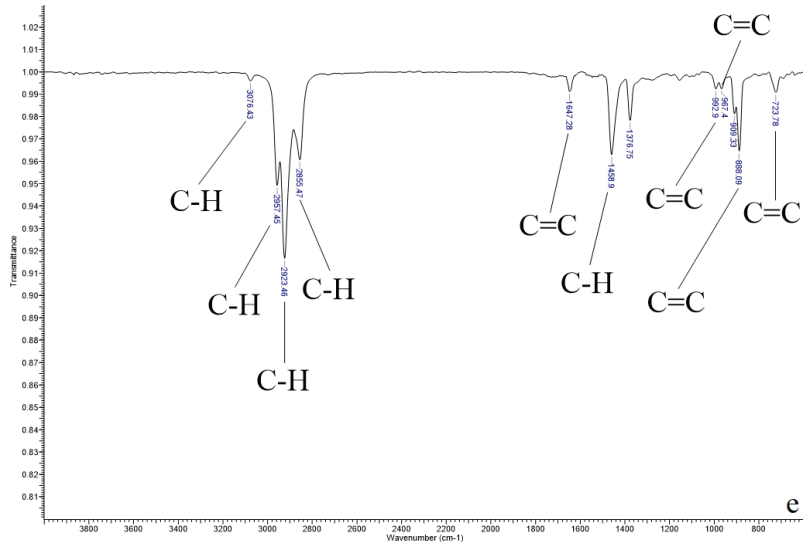


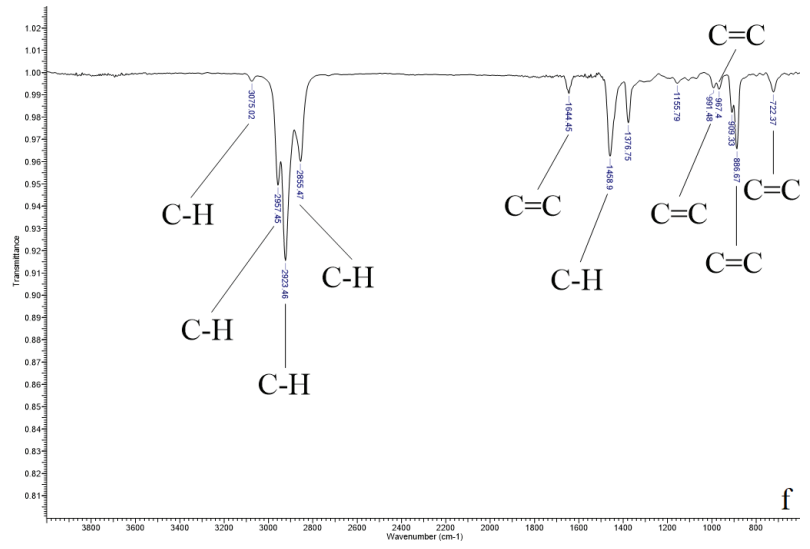


Figure 4.27 (cont.)

# CHAPTER 5

# CONCLUSION

Plastic packaging waste was collected and sorted during the pandemic period in İzmir. Model raw materials were prepared from virgin polyolefins based on the polyolefins that make up the majority of the plastic content. In this thesis, thermal and catalytic pyrolysis of this model polyolefin mixture (PO mixture) (42.4 wt.% PP, 40.5 wt.% HDPE and 17.1 wt.% LDPE) was investigated. Silica-alumina (Si/Al=30), silica-alumina (Si/Al=50), and ZSM-5 (Si/Al=50) supported silica-alumina (50) catalysts were produced by the sol-gel method.

The thermal pyrolysis of LDPE and PP plastics individually and of PO mixture in continuous set-up was investigated. The effects of parameters such as feeding rate (0.5 g/min-3 g/min), $N_2$ flow rate (800 mL/min -1100 mL/min), and condensation temperature (0 °C- (-25) °C) on product yield were observed. To observe the thermal pyrolysis behaviour of the PO mixture, an experiment was also conducted with the waste PO mixture (in the optimum conditions of 1100 mL/min $N_2$ flow rate and 1.5 g/min feeding rate). Virgin and waste pyrolysis oils were compared in terms of product yield and composition. 71.0 wt.% liquid, 22.4 wt.% gas and 6.6 wt.% solid-residue were obtained from the pyrolysis of virgin PO mixture. The liquid consisted of 54% gasoline, 38.5% diesel and 7.5% wax. As a result of the pyrolysis of waste PO mixture, 64.6 wt.% liquid, 28.7 wt.% gas and 6.8 wt.% solid-residue were obtained. The content of waste pyrolysis oil consisted of 38.2% gasoline, 45.5% diesel and 16.28% wax. In addition, 5-gram virgin PO mixtures were thermally pyrolyzed in a batch system with three different $N_2$ flow rates (100 mL/min, 150 mL/min, 200 mL/min). Under the influence of these three different $N_2$ flow rates, the liquid product was produced with a maximum of 57 wt.% with using 100 mL/min. 11.3 wt.% of the liquid yielded as wax and 45.7 wt.% as pyrolysis oil. When the chemical composition of pyrolysis oil was examined, 65.9% gasoline, 31.4% diesel and 2.7% wax were detected. It was observed that the most effective factor on the product yield among the examined process parameters was the $N_2$ flow rate.

In-situ catalytic pyrolysis of LDPE was performed with a batch operation to break down the waxy products to gasoline-diesel range. The amount and contents of the liquids obtained were compared by testing ZSM-5 (30) catalyst in four different catalyst-to-plastic ratios (1/100, 1/250, 1/500, 1/1000) and silica-alumina (30) 1/250 ratio. With a

catalyst-to-plastic ratio of 1/250, ZSM-5 (30) obtained 38.7 wt.% liquid with 88.2% gasoline, 10.2% diesel, and 1.6% wax content. Silica-alumina (30) produced 69.6 wt.% liquid with a content of 36.1% gasoline, 55.9% diesel, and 8.0% wax.

Three different catalysts (ZSM-5 (50), silica-alumina (50), ZSM-5 (50) supported silica-alumina (50)) and two different weight hourly space velocities, WHSV, (200 $h^{-1}$, 500 $h^{-1}$) were used for ex-situ catalytic pyrolysis with the $N_2$ flow rate of 100 mL/min. When ZSM-5 (50) catalyst was applied with 200 $h^{-1}$ WHSV, 29.9 wt.% liquid was produced with 82.9% gasoline, 16.7% diesel and 0.4% wax content, while with 500 $h^{-1}$ WHSV, 35.9 wt.% liquid produced in the content of 35.9% gasoline, 15.6% diesel and 4.1% wax. By using 200 $h^{-1}$ WHSV, silica-alumina (50) produced 54.1 wt.% liquid with the content of 65.8% gasoline, 28.3% diesel ve 5.9% wax, and by using 500 $h^{-1}$ WHSV, 56.6 wt.% liquid was produced with 66.2% gasoline, 31.2% diesel and 2.6% wax content. ZSM-5 (50) supported silica-alumina (50) with 200 $h^{-1}$ WHSV, 57.9 wt.% liquid obtained in the content of 63.8% gasoline, 30.7% diesel and 5.5% wax. And by using 500 $h^{-1}$ WHSV, 45.2 wt.% liquid was obtained with 65.0% gasoline, 30.7% diesel and 4.3% wax content.

FTIR and proximate & ultimate (elemental) analysis were applied to understand the composition and structure of waste and virgin polyolefins. TGA-DTG and DSC were applied to understand their thermal behaviour. The physicochemical properties of fresh catalysts were analyzed by FTIR and $NH_3$-TPD. Among the solid acid catalysts used in this work, it was detected that silica-alumina (50) and ZSM-5 supported silica-alumina (50) were weakly acidic and silica-alumina (30), ZSM-5 (30) and ZSM-5 (50) catalysts were strongly acidic. FTIR was also applied to spent catalysts to monitor coke formation. There were not any coke formation observed after the experiments ES3 and ES4 with silica-alumina (50) catalysts, and ES6 with ZSM-5 (50) supported silica-alumina (50). The content of liquid products was determined by GC-MS. It was also supported with the help of FTIR.

The aim of this research was to produce maximum liquid in the $C_5$-$C_{20}$ hydrocarbon range from the thermal and catalytic pyrolysis of polyolefins. It was promising that the produced silica-alumina based solid-acid catalysts work in accordance with this target. In addition, it can be further improved by adding support or promoters with metals such as Ni/Co on the catalysts. Also, catalyst regeneration should be studied. After that to improve this work, ex-situ catalytic pyrolysis should be performed on

continuous operation and system should be scaled up. Besides, the economic consideration and life cycle assessment of this work should be investigated.

# REFERENCES


A.G. Buekens, H. Huang. 1998. “Catalytic plastics cracking for recovery of gasoline-range hydrocarbons from municipal plastic wastes.” *Resources, Conservation and Recycling*, 163-181.

Chang, Siu Hua. 2023. “Plastic waste as pyrolysis feedstock for plastic oil production: A review.” *Science of The Total Environment*, 15 June: 1-18.

Charlotte Abdy, Yuqing Zhang, Jiawei Wang, Yang Yang, Ignacio Artamendi, Bob Allen. 2022. “Pyrolysis of polyolefin plastic waste and potential applications in asphalt road construction: A technical review.” *Resources, Conservation and Recycling*, May: 1-5.

D. P. Serrano, J. Aguado, and J. M. Escola. 2012. “Developing Advanced Catalysts for the Conversion of Polyolefinic.” *ACS Catalysis*, 1925.

Dong Liu, Peng Yuan, Hongmei Liu, Jingong Cai, Daoyong Tan, Hongping He, Jianxi Zhu, Tianhu Chen. 2013. “Quantitative characterization of the solid acidity of montmorillonite using combined FTIR and TPD based on the NH3 adsorption system.” *Applied Clay Science*, 13 August: 407-412.

Dylan Jubinville, Elnaz Esmizadeh, Sainiwetha Saikrishnan, Costas Tzoganakis, Tizazu Mekonnen. 2020. “A comprehensive review of global production and recycling methods of polyolefin (PO) based products and their post-recycling applications.” *Sustainable Materials and Technologies*, September: 1-5.

El-Haggar, Salah M. 2007. “Chapter 1 Current Practice and Future Sustainability.” In *Sustainable Industrial Design and Waste Management Cradle-to-cradle for Sustainable Development*, by Salah M. El-Haggar, 13-18. Elsevier.

Eurostat. 2020. *Energy, transport and environment statistics.* Statistics, Luxembourg: European Union.

F. Faisal, M.G. Rasul, M.I. Jahirul, D. Schaller. 2023. “Pyrolytic conversion of waste plastics to energy products: A review on yields, properties, and production costs.” *Science of The Total Environment*, 25 February: 8-11.

Fan Zhang, Yuting Zhao, Dandan Wang, Mengqin Yan, Jing Zhang, Pengyan Zhang, Tonggui Ding, Lei Chen, Chao Chen. 2021. “Current technologies for plastic waste treatment: A review.” *Journal of Cleaner Production*, 1-13.

Fatma Defne Çalık, Güray Yildiz. 2022. “Catalytic pyrolysis of low density polyethylene.” *Innovations – Sustainability – Modernity – Openness. Modern solutions in engineering.* Bialystok: Politechnika Bialostocka. 21-28.

Gartzen Lopez, Maite Artetxe, Maider Amutio, Javier Bilbao, Martin Olazar. 2017. “Thermochemical routes for the valorization of waste polyolefinic plastics to produce fuels and chemicals. A review.” *Renewable and Sustainable Energy Reviews*, 346-360.

Haoran Yuan, Chengyu Li, Rui Shan, Jun Zhang, Yufeng Wu, Yong Chen. 2022. “Recent developments on the zeolites catalyzed polyolefin plastics pyrolysis.” *Fuel Processing Technology*, 15 December: 1-5.

Ijaz Hussain, Saheed A Ganiyu, Hassan Alasiri, Khalid Alhooshani. 2022. “A state-of-the-art review on waste plastics-derived aviation fuel: Unveiling the heterogeneous catalytic systems and techno-economy feasibility of catalytic pyrolysis.” *Energy Conversion and Management*, 15 December: 13-18.

Ina Vollmer, Michael J. F. Jenks, Mark C. P. Roelands, Robin J. White, Toon van Harmelen, Paul de Wild, Gerard P. van der Laan, Florian Meirer, Jos T. F. Keurentjes, and Bert M. Weckhuysen. 2020. “Beyond Mechanical Recycling: Giving New Life to Plastic Waste.” *Angewandte Chemie International Edition*, 15416-15417.

Junya Nishino, Masaaki Itoh, Hironobu Fujiyoshi, Yoshio Uemichi. 2008. “Catalytic degradation of plastic waste into petrochemicals using Ga-ZSM-5.” *Fuel*, 3681-3686.

KO, E. I. 1997. “Chapter 2 Preparation of Solid Catalysts .” In *Handbook of Heterogeneous Catalysis* , by H. Knozinger, J. Weitkamp G. Ertl, 86-94. Wiley-VCH.

Landau, Miron V. 2009. “5 Sol-gel Processing.” In *Synthesis of Solid Catalysts*, by Krijn P. de Jong, 83-109. Wiley.

Lesli O. Mark, Melissa C. Cendejas, and Ive Hermans. 2020. “The Use of Heterogeneous Catalysis in the Chemical Valorization of Plastic Waste.” *ChemSusChem*, 5808-5836.

Liangliang Fan, Zheyang Su, Jiabo Wu, Zhiguo Xiao, Pei Huang, Lei Liu, Haiwei Jiang, Wenguang Zhou, Shiyu Liu, Roger Ruan. 2021. “Integrating continuous-stirred microwave pyrolysis with ex-situ catalytic upgrading for linear low-density

polyethylene conversion: Effects of parameter conditions." *Journal of Analytical and Applied Pyrolysis*, 21 May: 1-10.

Luis Noreña, Julia Aguilar, Violeta Mugica, Mirella Gutierrez and Miguel Torres. 2011. "Materials and Methods for the Chemical Catalytic Cracking of Plastic Waste." In *Material Recycling – Trends and Perspectives*. Mexico: www.intechopen.com.

M.I. Jahirul, M.G. Rasul, D. Schaller, M.M.K. Khan, M.M. Hasan, M.A. Hazrat. 2022. "Transport fuel from waste plastics pyrolysis – A review on technologies, challenges and opportunities." *Energy Conversion and Management*, 15 April: 1-12.

Martyna Solis, Semida Silveira. 2020. "Technologies for chemical recycling of household plastics – A technical review and TRL assessment." *Waste Management*, 128-138.

Marvin Kusenberg, Andreas Eschenbacher, Marko R. Djokic, Azd Zayoud, Kim Ragaert, Steven De Meester, Kevin M. Van Geem. 2022. "Opportunities and challenges for the application of post-consumer plastic waste pyrolysis oils as steam cracker feedstocks: To decontaminate or not to decontaminate?" *Waste Management*, 3 December: 83-93.

Mehrdad Seifali Abbas-Abadi, Yannick Ureel, Andreas Eschenbacher, Florence H. Vermeire, Robin John Varghese, Jogchum Oenema, Georgios D. Stefanidis, Kevin M. Van Geem. 2023. "Challenges and opportunities of light olefin production via thermal and catalytic pyrolysis of end-of-life polyolefins: Towards full recyclability." *Progress in Energy and Combustion Science*, May: 1-14.

Ministry of Environment, Urbanization and Climate Change-General Directorate of Environmental Management-Zero Waste and Waste Processing Department-Zero Waste Practices Branch Directorate. 2020. *PACKAGING BULLETIN, PACKAGING AND PACKAGING WASTE STATISTICS (2020).* Statistics, Ankara: Ministry of Environment, Urbanization and Climate Change-General Directorate of Environmental Management-.

Nan Zhou, Leilei Dai, Yuancai Lv, Hui Li, Wenyi Deng, Feiqiang Guo, Paul Chen, Hanwu Lei, Roger Ruan. 2021. "Catalytic pyrolysis of plastic wastes in a continuous microwave assisted pyrolysis system for fuel production." *Chemical Engineering Journal*, 20 March: 1-11.

PAGEV. 2020. *Türkiye plastics industry monitoring report.* Industry monitoring report, İstanbul: PAGEV.

PROVINCIAL DIRECTORATE OF ENVIRONMENT, URBANIZATION AND CLIMATE CHANGE. 2021. *IZMIR PROVINCE 2021 ENVIRONMENTAL REPORT.* Environmental report, İzmir: IZMIR GOVERNORSHIP.

R. Miandad, M.A. Barakat, Asad S. Aburiazaiza, M. Rehan, I.M.I. Ismail, A.S. Nizami. 2017. "Effect of plastic waste types on pyrolysis liquid oil." *International Biodeterioration & Biodegradation*, 239-242.

S. Kartik, Hemant Kumar Balsora, Manisha Sharma, Agus Saptoro, Rakesh K. Jain, Jyeshtharaj B. Joshi, Abhishek Sharma. 2022. "Valorization of plastic wastes for production of fuels and value-added chemicals through pyrolysis – A review." *Thermal Science and Engineering Progress*, 1 July: 10-15.

S.L. Wong, N.Ngadi, T.A.T.Abdullah, I.M.Inuwa. 2015. "Current state and future prospects of plastic waste as source of fuel: A review." *Renewable and Sustainable Energy Reviews*, 9 June: 1167-1174.

Sachin Kumar, Achyut K. Panda, R.K. Singh. 2011. "A review on tertiary recycling of high-density polyethylene to fuel." *Resources, Conservation and Recycling*, 904-907.

Sakthipriya, Nallusamy. 2022. "Plastic waste management: A road map to achieve circular economy and recent innovations in pyrolysis." *Science of the Total Environment*, 22 October: 1-5.

Seyed Amir Hossein Seyed Mousavi, Seyed Mojtaba Sadrameli, Amir Hossein Seedi Dehaghani. 2022. "Catalytic pyrolysis of municipal plastic waste over nano MIL-53 (Cu) derived @ zeolite Y for gasoline, jet fuel, and diesel range fuel production." *Process Safety and Environmental Protection*, 15 June: 449-467.

Tu Xayachak, Nawshad Haque, Raj Parthasarathy, Sarah King, Nargessadat Emami, Deborah Lau, Biplob Kumar Pramanik. 2022. "Pyrolysis for plastic waste management: An engineering perspective." *Journal of Environmental Chemical Engineering*, December: 1-11.

Vahid Mortezaeikia, Omid Tavakoli, Mohammad Saleh Khodaparasti. 2021. "A review on kinetic study approach for pyrolysis of plastic wastes using thermogravimetric analysis." *Journal of Analytical and Applied Pyrolysis*, November: 1-7.

Yihan Wang, Kai Wu, Siyu Wang, Jiajun Yu, Bingbing Luo, Huiyan Zhang. 2023. "Tandem catalytic pyrolysis of mixed plastic packaging wastes to produce BTEX over dual catalysts." *Fuel Processing Technology*, May: 7-8.

Yildiz G., Ronsse F. And Prins W. 2017. “Catalytic Fast Pyrolysis Over Zeolites.” In *Fast Pyrolysis of Biomass: Advances in Science and Technology*, 200-230.

Yujie Peng, Yunpu Wang, Linyao Ke, Leilei Dai, Qiuhao Wu, Kirk Cobb, Yuan Zeng, Rongge Zou, Yuhuan Liu, Roger Ruan. 2022. “A review on catalytic pyrolysis of plastic wastes to high-value products.” *Energy Conversion and Management*, 115243.